Palaeogeography, Palaeoclimatology, Palaeoecology 700 (2026) 114071

Contents lists available at ScienceDirect

Palaeogeography, Palaeoclimatology, Palaeoecology

journal homepage: www.elsevier.com/locate/palaeo

Upper Tortonian skeletal assemblages of phosphatic hardgrounds record upwelling pulses and internal-wave processes (Latium–Abruzzi Platform, Italy)☆

Daniela Basso [a,*], Valentina Alice Bracchi [a], Irene Cornacchia [b], Alessandro Mancini [c], Marco Brandano [c]

[a] Dipartimento di Scienze dell'Ambiente e della Terra, Università di Milano-Bicocca, Piazza della Scienza 4, 20126 Milano, Italy
[b] Istituto di Geologia Ambientale e Geoingegneria (IGAG), Consiglio Nazionale delle Ricerche (CNR), Università Sapienza, P.le Aldo Moro, 5, 00185 Roma, Italy
[c] Dipartimento di Scienze della Terra, SAPIENZA Università di Roma, P.le Aldo Moro, 5, 00185 Roma, Italy

ARTICLE INFO

Editor: L Angiolini

Keywords:
Tortonian rhodoliths
coralline algae
bryozoans
acervulinids
upwelling variability
internal waves

ABSTRACT

Miocene hardgrounds of the circum-Mediterranean region are widely interpreted as records of upwelling of nutrient-rich water, commonly associated with phosphatization along platform margins. On the Latium–Abruzzi Platform, the Sirente Mt. and Tornimparte successions document two distinct phosphatic intervals: in situ authigenic hardgrounds and reworked phosphate-rich deposits, respectively. At Tornimparte, phosphorite beds are interpreted as the product of gravity flows triggered by internal-wave breaking along a density-stratified outer ramp. Erosion of a phosphatization zone generated lithoclasts that were transported basinward and redeposited chaotically, as supported by taphonomic evidence and CT-scan analyses of macrofossil-bearing blocks. The in situ deposits of Sirente Mt. represent fossil rhodolith beds, dominated by boxwork morphotypes, and composed chiefly of coralline algae of the genus *Mesophyllum*, with subordinate *Lithothamnion*, encrusting bryozoans, acervulinids, and serpulids. Their loose internal structure, multispecific encrustations, and fine sediment infill indicate low-energy conditions and relative substrate stability. Taxonomic composition, absence of shallow-water coral taxa, and dominance of thin hapalidialean thalli suggest development on a deep tropical oligophotic ramp (ca. 70–100 m). Growth-rate contrasts between slow-growing corallines and faster bryozoans, together with alternating algal- and bryozoan-dominated layers observed in rhodoliths, imply multiannual fluctuations in nutrient supply rather than simple seasonal forcing. Upwelling-driven nutrient enrichment likely enhanced phytoplankton productivity, turbidity, and pCO_2, periodically favoring suspension feeders over coralline algae in a context of intense space competition. These cyclical ecological shifts recorded in rhodoliths may reflect interannual to decadal variability in wind-driven upwelling intensity, consistent with broader Tortonian paleoceanographic perturbations. Collectively, sedimentological, compositional, and taphonomic evidence supports a dynamic outer-ramp system modulated by recurrent upwelling pulses and possible internal-wave processes.

1. Introduction

The Central Apennines (Italy) are largely composed of carbonate rocks belonging to the extensive Latium–Abruzzi and Apula Platforms. The Miocene Mediterranean carbonate successions of the Apennines record drowning carbonate platforms and depositional hiatuses associated with phosphate-rich hardgrounds (Föllmi et al., 2008, 2015). Hardgrounds are the result of seafloor lithification through cementation occurring at the sediment–water interface, by carbonate minerals and other phases, such as glauconite, phosphate, and iron oxides. Hardgrounds can also occur as components of condensed beds or form highly condensed horizons independently (Föllmi, 2016). Sedimentary condensation, as described by Föllmi (2016), develops within hydrodynamically active settings capable of winnowing, eroding, reworking,

☆ This article is part of a Special issue entitled: 'Mediterranean Miocene' published in Palaeogeography, Palaeoclimatology, Palaeoecology.

* Corresponding author.
E-mail addresses: daniela.basso@unimib.it (D. Basso), valentina.bracchi@unimib.it (V.A. Bracchi), irene.cornacchia@igag.cnr.it (I. Cornacchia), a.mancini@uniroma1.it (A. Mancini), marco.brandano@uniroma1.it (M. Brandano).

https://doi.org/10.1016/j.palaeo.2026.114071
Received 15 February 2026; Received in revised form 14 July 2026; Accepted 15 July 2026
Available online 16 July 2026
0031-0182/© 2026 The Authors. Published by Elsevier B.V. This is an open access article under the CC BY-NC-ND license (http://creativecommons.org/licenses/by-nc-nd/4.0/).

and bypassing sediments, while simultaneously promoting authigenic processes. Such regimes may involve persistently high energy conditions, typical of current-dominated environments, or intermittent, high-energy events such as storms or turbidity currents. Sediment supply can be continuous or episodic, often linked to gravity flows or storm-driven deposition. These conditions produce a long-lasting, dynamic balance among sediment deposition, erosion and winnowing, and authigenic formation over geologically significant periods (Purser, 1969; Wilson, 1975; Mutti and Bernoulli, 2003; Föllmi, 2016). Nevertheless, not all intervals of starved sedimentation lead to hardground development, indicating the influence of complex and highly variable controls that have changed markedly and repeatedly over the Phanerozoic (Christ et al., 2015). Owing to their genetic association with reduced sediment supply, hardgrounds are commonly linked to maximum regression surfaces or drowning unconformities during phases of relative sea-level rise (Loutit et al., 1988; Mutti and Bernoulli, 2003; Föllmi et al., 2011; Yilmaz et al., 2012). Sea-level fluctuations are in turn related to major climatic shifts influencing the rate of carbonate production and/or accumulation (Godet et al., 2013; Brigaud et al., 2014). In modern warm, shallow tropical seas with high $CaCO_3$ saturation, early seafloor cementation and hardground formation are common, but small variations in bathymetry, substrate, hydrodynamics, and sedimentation–erosion balance produce spatially variable petrological properties (Christ et al., 2015). In heterozoan carbonate platforms, such as the Oligo-Miocene carbonate ramps of the Mediterranean (Mutti and Bernoulli, 2003; Christ et al., 2015) hardground formation is less common, and locally favoured by active seawater circulation associated with those factors that may enhance carbonate saturation, such as the oxidation of methane associated with sulfate reduction, or the microbial activity linked to the decay of organic matter at the seafloor (Garrison et al., 1969; Corselli et al., 1994; Torres et al., 2009).

Hardgrounds may preserve and host a diverse biota, allowing for paleoenvironmental reconstruction. During their formation, hardgrounds lithify the pre-existing sediment with its biogenic content. The hardground exposure on the seafloor allows later colonization by active biological communities whose living components may leave behind distinct bioerosion marks and encrustations. Both features may be subsequently preserved in the rock record, providing critical evidence for paleoenvironmental reconstruction. For example, Tortonian hardgrounds in Menorca (Spain) have been estimated as formed at water depths of $<$100 m, based on benthic foraminifers and coralline algae (Brandano et al., 2016), while Pleistocene Italian examples, as well as the Upper Cretaceous chalk hardgrounds of southern England, indicate outer-shelf formation (Kennedy and Garrison, 1975; Corselli et al., 1994). Modern analogs demonstrate that hardgrounds can also form on continental slopes (hundreds to $>$1000 m) under sediment starvation and substrate exposure (Chen et al., 2025). These observations highlight that hardground formation is controlled more by sedimentation rates, nutrient flux, and bottom-water circulation than by absolute depth, and that fossil assemblages associated with hardgrounds can provide critical constraints in paleodepth reconstruction.

Phosphatic hardgrounds, commonly cemented by fluoroapatite at or near the sediment–water interface, are especially valuable as multi-proxy archives, integrating sedimentological, geochemical, and paleontological signals (Glenn and Arthur, 1988; Christ et al., 2015; Föllmi, 1996; Föllmi et al., 2008, 2015). Their formation is governed by low sedimentation rates, early authigenic mineral precipitation driven by organic matter remineralization, and bottom-current activity, all of which are modulated by regional and global oceanographic factors such as nutrient availability, carbonate saturation state, and circulation patterns (Brandano et al., 2016; Cornacchia et al., 2022).

Miocene phosphatic hardgrounds are widely documented across the central Mediterranean, forming 10–20 cm thick layers enriched in phosphate, glauconite, and macrofossils. Paleontological analyses show that in most cases these horizons host sclerobiont communities (Taylor and Wilson, 2002) dominated by suspension-feeders, indicating mesotrophic to eutrophic conditions, moderate to strong bottom currents, and relatively deep, low-light environments (~100–350 m). Multi-phase encrustation and bioerosion traces (ichnogenera *Trypanites*, *Gastrochaenolites*, *Entobia*) indicate prolonged seafloor exposure and episodic colonization, making these deposits time-averaged, condensed ecological archives (Vescogni et al., 2018; Rehfeld and Janssen, 1995). Geochemical data, including neodymium isotopes indicate that phosphate-rich waters formed under conditions of weakened Mediterranean circulation, limited exchange with Atlantic surface waters, and enhanced upwelling of nutrient-rich deep waters, which brought dissolved phosphate in the photic zone seafloor, where it could precipitate as phosphatic hardgrounds. In this model (Cornacchia et al., 2022) the primary controls on Mediterranean Middle to Late Miocene phosphogenesis were upwelling and nutrient supply driven by regional oceanographic changes linked to global climate shifts and basin circulation evolution.

In the Miocene of the Apennines, it has been demonstrated that hardground formation within the succession of the Maiella ramp, northern extension of Apula Platform, was related to upwelling fluxes, likely induced by regional changes in water circulation and modulated by sea-level fluctuations and enhanced biological productivity (Mutti and Bernoulli, 2003). Although the role of upwelling in hardground formation is largely recognized, a more precise paleoenvironmental reconstruction of the plausible paleodepth reached by the upwelled water mass is seldom available.

Tortonian to lower Messinian phosphatic hardground formation is recorded on top of the Latium-Abruzzi carbonate ramp succession, where the occurrence of this phosphate-bearing surfaces and deposits marks the drowning of the platform due to regional and global causes (Brandano et al., 2020). In this study, two outcrops were investigated, representative of two different situations and processes. The Sirente Mountain hardground developed as an authigenic, phosphate-rich surface on top of a middle-ramp environment (Brandano et al., 2009). In contrast, the Tornimparte outcrop exposes a phosphatic interval located between the uppermost outer-ramp carbonate deposits and the overlying hemipelagic marls. At Tornimparte, this interval is interpreted as the result of the dismantling of a phosphatic hardground and includes phosphatic lithoclasts together with a rich autochthonous and allochthonous fauna (Brandano et al., 2020). Thus, the two outcrops were chosen since they developed at different depths and in different hydrodynamic settings, but were both affected by the upwelling of P-rich waters that led to hardground formation. The skeletal assemblage at Tornimparte is dominated by mollusks, isolated corals, and shark teeth; however, the provenance of this assemblage has not previously been analysed. In the Sirente Mt., the top of carbonate ramp succession is dominated by rhodolith rudstone, drowned and overlaid by a hemipelagic clayey marlstone rich in planktonic foraminifera (Brandano et al., 2009). Rhodolith structure and composition collectively mirror the paleoenvironmental conditions in which rhodoliths developed, in some cases recording the succession of temporally distant, separate phases of growth (Basso and Tomaselli, 1994; Basso et al., 1998; Nebelsick et al., 2013; Vale et al., 2018; Bracchi et al., 2019). Fossil assemblages and sedimentary facies of the Sirente Mt. hardground suggest formation in mid-ramp paleoenvironments, however, a more precise paleoenvironmental reconstruction is still lacking. The paleoecological analysis of the fossil benthic assemblages at Tornimparte and the Sirente Mt. rhodoliths provides an opportunity to explore the Tortonian benthic environments affected by phosphatization and hardground formation, thereby filling a gap in the literature. Although these surfaces have been extensively studied using sedimentological and mineralogical approaches (Brandano et al., 2009, 2020), as well as from a paleoceanographic perspective (Cornacchia et al., 2022), critical questions regarding the seafloor environments and the biota that underwent hardground formation remain unresolved within the context of benthic paleoecology. The aims of this paper are: 1) using the paleoenvironmental approach to assess the paleodepth reached by the

upwelling P-rich waters responsible for the hardground formation, and 2) exploring the possibility that some evidence of the Tortonian environmental conditions triggering hardground formation could be detected in the affected benthic facies, in terms of skeletal components, taphonomy, and species association.

2. Geological setting

The Italian Apennines represent a fold-and thrust belt derived from Neogene deformation of the Tethys passive margin. The evolution of the Apennine chain is related to the west-directed subduction of the Adriatic

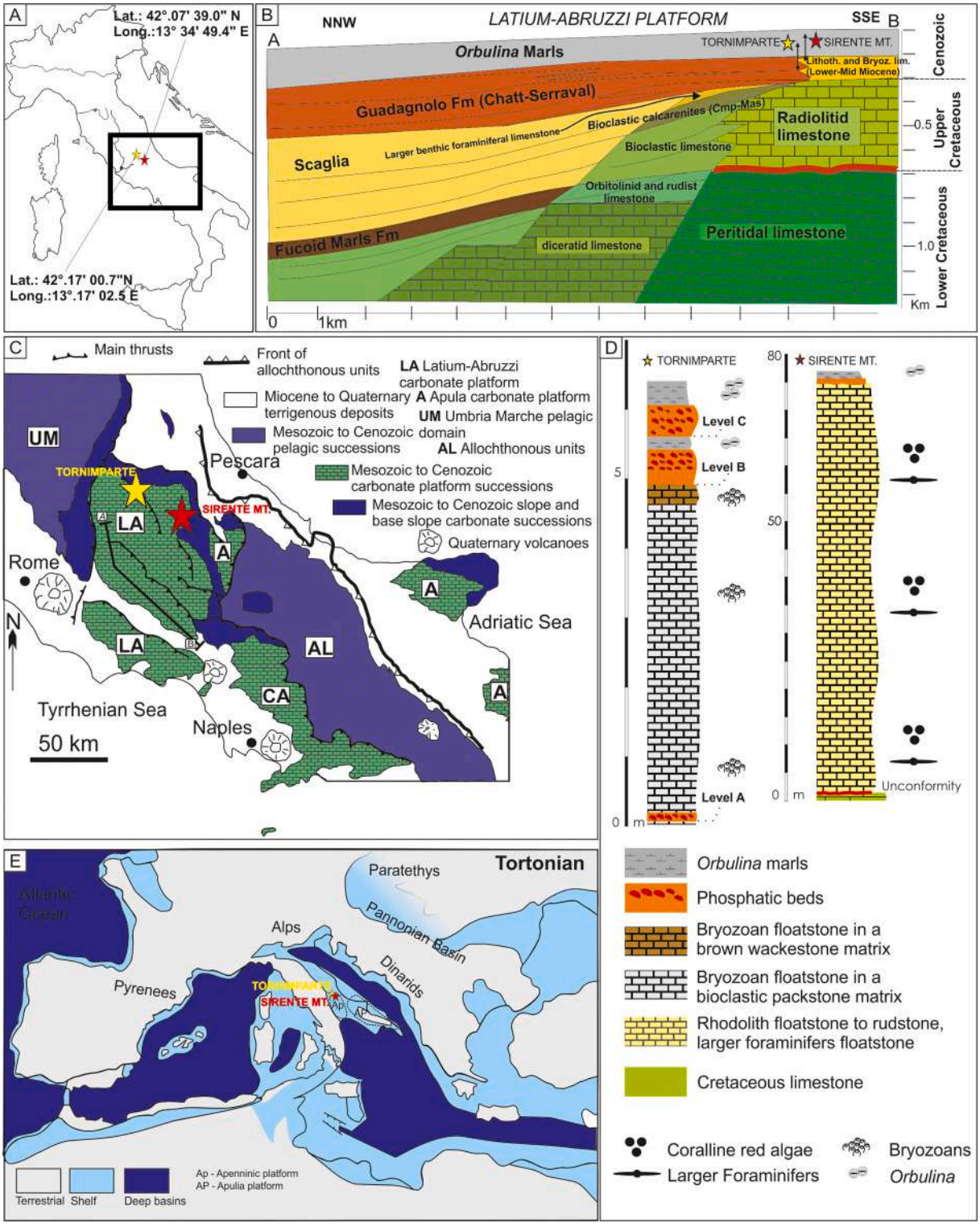


Fig. 1. A: study sites in central Italy (yellow star: Tornimparte; red star: Sirente Mt.). B: stratigraphic architecture of the Latium Abruzzi platform and the transition to the Umbria-Sabina Basin with the position of the two stratigraphic sections. C – D: schematic geological map of central Italy and the stratigraphic sections of Tornimparte and Sirente Mt. (D), showing the position of the phosphatic levels investigated (modified from Brandano et al., 2020). E: Mediterranean paleogeography during the Tortonian (modified from Cornacchia et al., 2022). (For interpretation of the references to colour in this figure legend, the reader is referred to the web version of this article.)

plate under the European plate (e.g. Doglioni, 1991). The Neogene to Recent evolution of the north-central Apennines is characterized by east-north-eastward migration of deformation fronts and related foredeeps (Ricci Lucchi, 1986; Patacca and Scandone, 1989).

In central Apennines, the Latium-Abruzzi succession crops out (Fig. 1A). The passive margin sediments of the Latium-Abruzzi platform mainly consist of Upper Triassic-Upper Miocene succession of shallow-water carbonates deposited in a tropical to subtropical environment. The Cretaceous platform limestones are unconformably overlain by the Cenozoic portion of the platform, represented almost exclusively by Miocene limestones, belonging to the "Calcari a Briozoi e Litotamni" Formation (CBL = Bryozoan and *Lithothamnion* limestones Fm) (Damiani et al., 1992; Civitelli and Brandano, 2005) (Fig. 1B-C). Miocene carbonates are dated to the Burdigalian–Tortonian (Brandano, 2002; Civitelli and Brandano, 2005; Brandano, 2017; Brandano et al., 2010, 2017), when the CBL accumulated on a low-angle homoclinal ramp, resulting both from the inherited Cretaceous carbonate substratum and from the locus of carbonate production and accumulation, under persistent subtropical conditions.

Along the Latium-Abruzzi carbonate ramp, three depositional environments can be identified within the CBL: the inner portion was characterized by a high-energy littoral environment, passing into a shallow-water euphotic zone represented by seagrass-meadows interbedded with free-living, branching red algae facies ("Mäerl" facies), at water-depths of a few tens of meters (Brandano, 2003). Small and scattered coral mounds marked the transition to the middle ramp environment. In the middle ramp, developed in the oligophotic zone (Pomar, 2001), rhodoliths and larger benthic foraminifera (*Heterostegina*, *Operculina*, *Amphistegina*) dominated the carbonate production, with subordinate echinoids, bryozoans and bivalves (rhodalgal lithofacies, sensu Carannante et al., 1988). In the outer ramp the bryomol (sensu Nelson, 1988) and molechfor (sensu Carannante et al., 1988) lithofacies dominated in the aphotic zone (Corda and Brandano, 2003; Brandano et al., 2010). In the external outer-ramp belt, siliceous sponge spicules, echinoid fragments, and planktonic foraminifera are the main sediment components.

The eastward migrating thrust belt-foredeep system controlled a diachronous marine transgression induced by tectonic subsidence (Brandano and Corda, 2002), which terminated the carbonate deposition by Late Miocene time, due to plate flexure-related drowning and coeval increasing input of siliciclastic sedimentation. According to the diachronic carbonate facies deposition controlled by the migrating thrust belt-foredeep system, the resumed Miocene carbonate production above the Cretaceous unconformity has been dated at 19–18 Ma at its base (Brandano et al., 2017), and 15–16 Ma on top in the southwestern sectors, while in the eastern sectors (Marsica, Sirente Mt), the rhodolithic unit was dated at 15–16 Ma and the top at 11–9 Ma (Brandano, 2002). The end of the carbonate sedimentation as well as the age of the terrigeneous deposits are progressively younger moving north-eastward, also as result of the Late Miocene evolution of the thrust-belt foredeep system (Cipollari and Cosentino, 1995).

The phosphatic hardgrounds developed on top of the Miocene carbonate ramp succession and mark the end of the shallow-water deposition (Fig. 1D-E). The hardgrounds are overlaid by the hemipelagic clayey marlstone known as *Orbulina* marls unit, which documents two major steps in the geodynamic evolution of the Central Apennines: the drowning of the carbonate platform and the beginning of synorogenic turbiditic siliciclastic deposition (Pampaloni et al., 1994).

In the Carseolani Mountains the marls immediately overlying the hardground have been dated by Pampaloni et al. (1994) and Cosentino et al. (1997) as belonging to the CN8 Nannofossil zone (9–9.5 Ma, late Tortonian).

In the central Apennines, phosphatic hardgrounds from Sirente Mt., and Tornimparte in the uppermost member of the Guadagnolo Formation (Brandano et al., 2020; Fig. 1B-D), follow the Monterey Event (Early–Middle Miocene, ~17–13 Ma), and the Mid-Miocene Climatic Optimum (between 17.0 Ma and 13.5 Ma), recording a global positive carbon isotope excursion associated with increased marine productivity. Enhanced nutrient availability, massive organic carbon burial, intensified oceanic circulation are linked with the increased productivity in the context of the carbonate platform drowning (Föllmi et al., 1994; Wissler et al., 2003; Weissert and Erba, 2004; Brandano et al., 2017).

3. Material and methods

The rhodolith rudstone outcropping on the Sirente Mt. (Prato di Popolo, m 1630) was sampled at the top of the succession, where the hardground lays at the ground level, and just below the phosphatic hardground. Representative rhodolith-rich samples were randomly collected within the same stratigraphic level along a 4 m line, and transported to the facilities of the Milano-Bicocca University, where they have been cut by a rock saw. One or two thin sections were prepared from each rhodolith. Other thin sections belonging to the Brandano collection, and obtained from rhodoliths collected at the same outcrop and levels, were included in this study. A total of twenty thin sections were then examined at the University of Milano-Bicocca under a transmitted light optical microscope to analyze the components and identify the fossil coralline algae at the lowest possible taxonomic rank. Point counting provides useful results for describing the mean contribution of the different components of rocks (Flügel, 2010, pp. 254–258). The component analysis of rhodoliths was based on 300 point counting of the standard-sized petrographic thin sections (2.8 × 4.6 cm). The categories of biogenic constituents considered for the percentage quantification were: coralline red algae, benthic and planktonic foraminifera, corals (later excluded because not observed), annelids, mollusks, brachiopods, bryozoans, crustaceans, echinoderms, micrite, cement, authigenic minerals. Identification of coralline algae was performed under OM higher magnification (up to x200). Coralline red algae taxonomy follows AlgaeBase (Guiry and Guiry, 2026). Identification in fossil material is based on Braga (2003) and Hrabovský et al. (2016). Coralline algal growth-form terminology follows Woelkerling et al. (1993). Sphericity (Sneed and Folk, 1958) was not calculated due to the impossibility to properly isolate integer rhodoliths from the rock, but was qualitatively obtained from field observations and hand samples. Animal taxonomy follows WoRMS (2026).

At Tornimparte, two blocks measuring 15–20 cm and 30 samples measuring 3–5 cm were collected from the last of the two phosphatic intervals outcropping in the area (Brandano et al., 2020; figs. S2D, S4 in Cornacchia et al., 2022). This interval corresponds to a grain-supported conglomerate ranging from 10 to 15 cm in thickness that occurs with a grey to brownish packstone to wackestone matrix.

The two large blocks collected at Tornimparte were analysed using a CT scan with the Revolution EVO, which is integrated with the PET/CT Discovery MI scanner (General Electric), owned by "Fondazione Tecnomed" at the University of Milano-Bicocca and located in the Nuclear Medicine Department in Monza, Italy. The acquisition parameters were as follows: 140 kV and a step size of 0.625 mm. The blocks were scanned along their three main axes, and the images were reconstructed using the "bone plus" axial filter to best visualise the inner structure. The results yielded tomographic images of the blocks in greyscale, reflecting the varying densities of the inner structure, using AMIRA-Avizo software (Thermo Fisher Scientific).

The hand samples containing fossils were primarily observed and photographed under a binocular microscope. After preliminary observation, some samples were reduced to a minimum size around the fossil particles and placed in 80% acetic acid for at least two hours to extract fossils. When needed, final manual polishing of the fossil surface was made using a hand micro-drill.

Additionally, 11 standard-sized petrographic thin sections (2.8 × 4.6 cm) were prepared from some samples to describe the inner components, based on 300-point counting. The categories of the constituents considered for the percentage quantification were: benthic foraminifera,

corals, bryozoans, mollusks, echinoderms, coralline algae, glauconitic wackestone with planktonic foraminifera, wackestone with planktonic foraminifera and phosphatized pebbles.

4. Results

4.1. The rhodoliths of Sirente Mt

The field observations and the paleontological analysis revealed that rhodoliths were packed and embedded in poorly sorted packstone-wackestone with fragments of bryozoans, echinoderms, mollusks, crustaceans, annelid tubes and small benthic foraminifera (Figs. 2–4). The poorly sorted packstone-wackestone embedding the rhodoliths appears in contact with the coralline thalli, filling also the largest shelter porosity of the rhodoliths framework (Fig. 4A, E, I). Rhodoliths have a subspheroidal to ellipsoidal shape and a long axis spanning 4–10 cm (Fig. 2). The internal structure of rhodoliths shows multiple nuclei composed of bryozoan colonies or acervulinid foraminifera, overgrown by loosely superposed, thin laminar thalli of coralline algae (Figs. 2D–F and 4C–G). The microscopic primary porosity between algal thalli and inside the bryozoan colonies is filled by micrite, also with clotted fabric (Fig. 4J), containing only random and rare small benthic foraminifera, mainly belonging to the Subclass Textulariana. Rare, poorly preserved rotaliids occur in the internal bioclastic micrite of a few rhodoliths (including buliminoids), and large benthic foraminifera are exclusively represented by very rare fragments of *Heterostegina*.

Other porosity and fractures in connection with the rhodoliths surface is filled by glauconitic *Orbulina* marls unit (Fig. 4B,I). Corals were not detected in the studied material.

The coralline algal association of the examined rhodoliths (Fig. 3) is frequently represented by sterile thalli, less than 200 μm thick (Fig. 4A, F, G). Despite the rarity of diagnostic reproductive structures, most of the preserved material shows cell fusions, coaxial or non-coaxial plumose hypothallus and multiporate conceptacles, indicating that the studied rhodoliths are composed almost exclusively by Hapalidiales. In particular, the genus *Mesophyllum* is the most common, with abundant sterile thalli and some fertile specimens belonging to the species *Mesophyllum sancti-dionysii* Lemoine, 1939 (Fig. 4G-H) and *Mesophyllum*

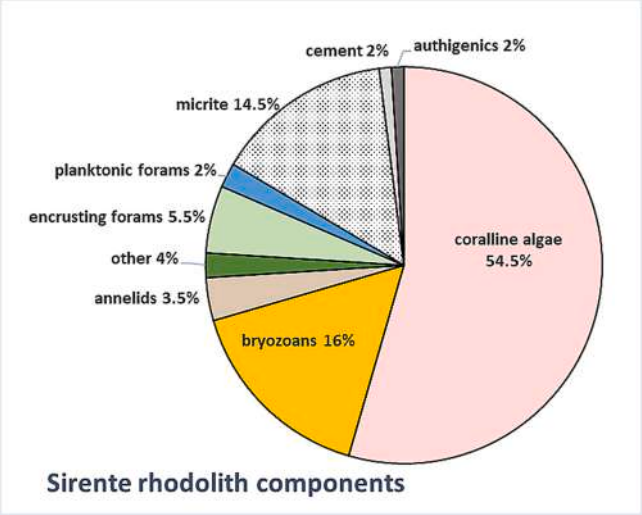


Fig. 3. Sirente rhodoliths. Pie chart showing the mean contribution of the different categories to the rhodoliths composition. Data from point counting. The category "other" groups the components with a mean contribution <1% (brachiopods, crustaceans, mollusks, echinoderms, non-encrusting benthic foraminifera).

curtum Lemoine, 1939 (Fig. 4J-K). Rhodolith corallines belonging to the genus *Lithothamnion/Phymatolithon* appear as a minor component of the Sirente rhodoliths (Fig. 4L). One single fertile thallus with uniporate conceptacles was observed, showing cell fusions and a coaxial hypothallus, that might belong to a yet undescribed gametangial phase of *Mesophyllum*, based on the similarity with extant examples and the correspondence of its vegetative characters with other co-occurring asexuate *Mesophyllum* plants.

Encrusting cheilostome bryozoans were frequently observed, growing directly over the corallines or directly overgrown by them. Tiny cyclostome bryozoan colonies were also randomly detected (Fig. 4). In some rhodoliths the encrusting bryozoan colonies appear interposed between algal laminar thalli in an almost cyclical and regular pattern. In

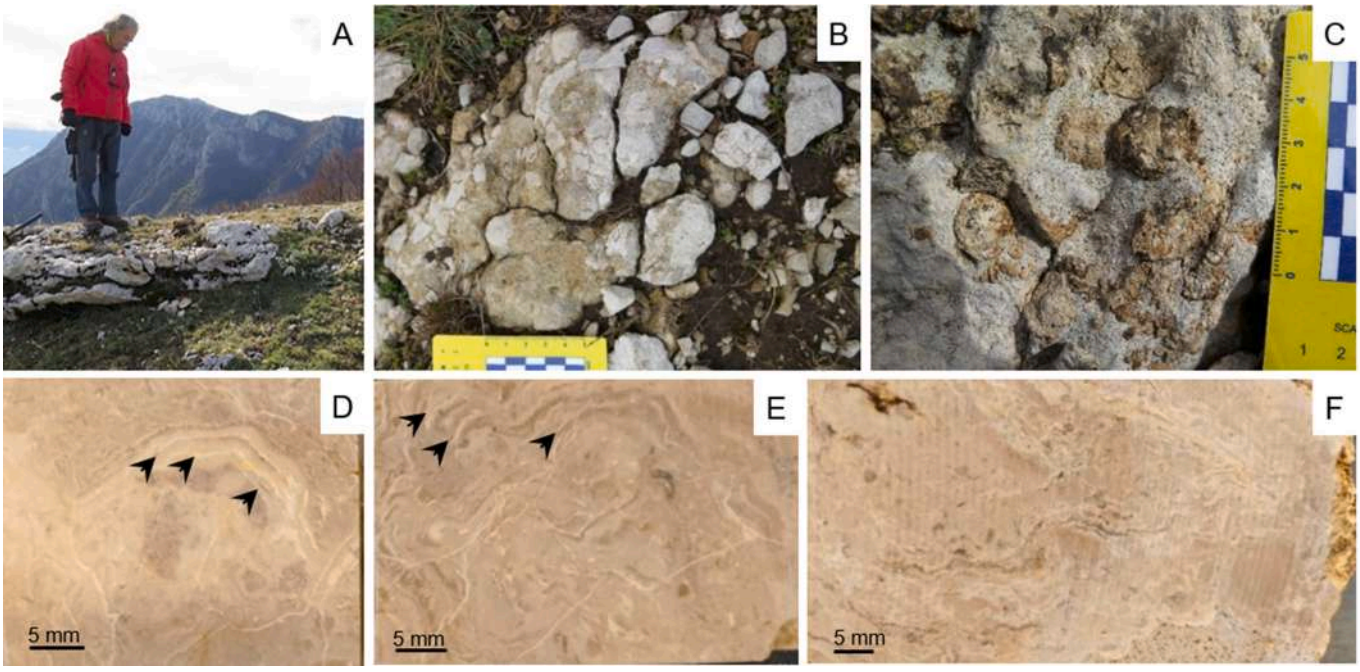


Fig. 2. Sirente Mt. A-C: the top of the Sirente Mt. succession and field views of the rhodolith rudstone outcrop. D-F: the internal structure of three spheroidal to ellipsoidal rhodoliths. Note the absence of obvious nuclei, the thin layering, and the rhythmic superposition of layers (arrowheads in D and E).

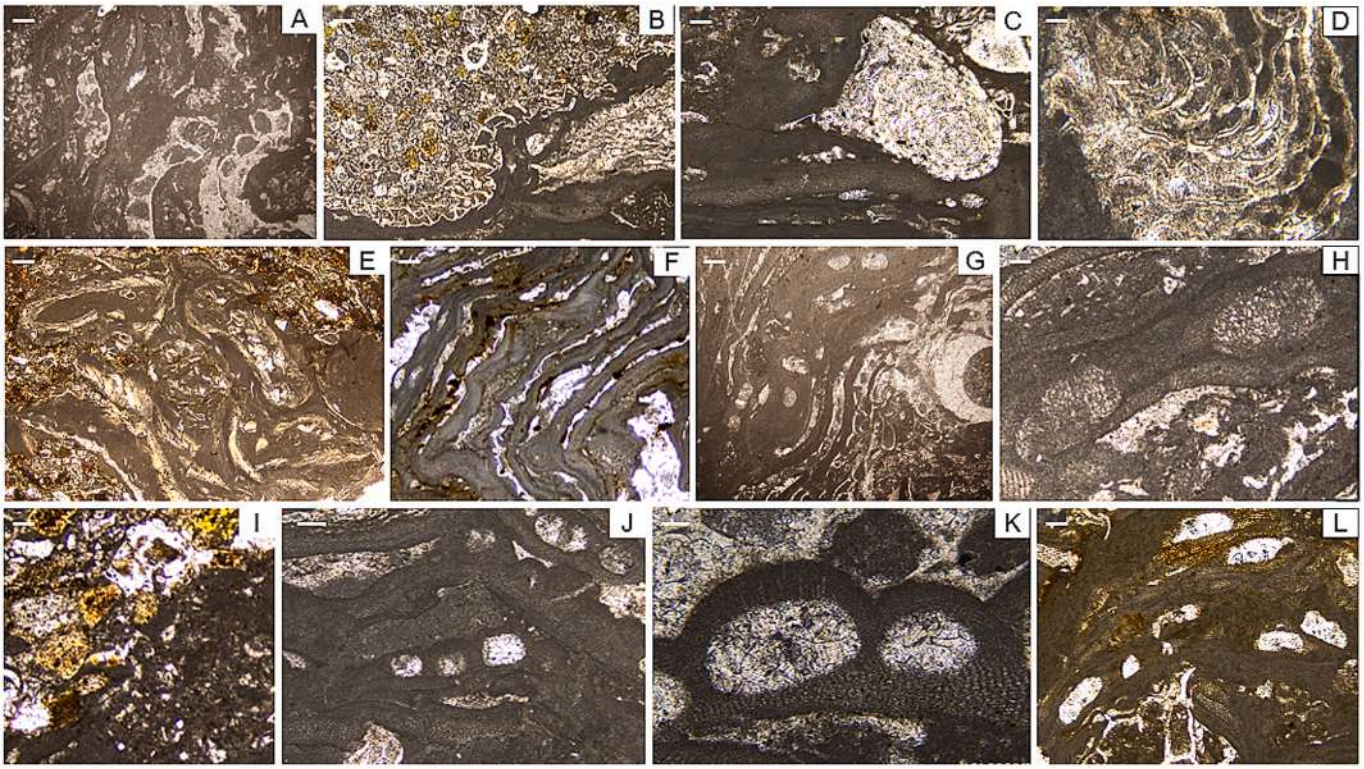


Fig. 4. Sirente rhodoliths. A: alternating and superposed generations of cheilostome bryozoans and laminar thalli of coralline algae (sample SIR 1F III, scale bar = 400 μm). B: a bryozoan colony encrusting coralline algae at the surface of a rhodoliths. Note the contact with the *Orbulina* marls unit (sample R4, scale bar = 400 μm). C: acervulinid micronodule encrusted by coralline algae (sample R11, scale bar = 200 μm). D: acervulinid (sample R7, scale bar =100 μm). E: aggregation of annelid tubes (sample R11, scale bar = 400 μm). F: alternation of coralline-dominated and bryozoan-dominated layers. Note that also dark-stained diagenetic levels, formed preferably along porosities, appear cyclical (sample R11, scale bar = 400 μm). G: from right to left, superposition of serpulid tubes, cheilostome bryozoan colonies, and laminar *Mesophyllum sancti-dionysii* thalli (sample SIR 1, scale bar = 400 μm). H: magnification of the multiporate conceptacles of *Mesophyllum sancti-dionysii,* typically filled by irregular sterile cells (sample R6, scale bar = 200 μm). I: contact between the authigenics-rich *Orbulina* marls unit (on left) covering the drowned rhodolith bed, and the bioclastic micrite (on right) embedding the rhodoliths during their growth (sample R11, scale bar = 100 μm). J: superposed thalli of *Mesophyllum curtum.* At the centre, note the absence of bioclasts in the micrite that partially fills the shelter porosity. Above, micrite overlaid by chalcedony, formed after diagenesis of a spicule-rich void (sample R7, scale bar = 200 μm). K: magnification of the conceptacle chambers of *Mesophyllum curtum* (sample R7, scale bar = 100 μm). L: an algal protuberance made of an unidentified hapalidiacean, showing numerous multiporate conceptacle chambers (sample R3, scale bar = 200 μm).

these cases, algal thalli have a thickness of about 200–400 μm, and obvious bryozoan colonies appear cyclically, approximately every 700–1500 μm (Figs. 2D-E, 4F), while minor interruptions of the algal growth appear to correspond to micrite filling, frequently associated to dark staining. No obvious pattern of change in component association could be detected through an ideal transect from the inner to the outer portion of the examined rhodoliths. Obvious nuclei of first encrustation were not identified, however, acervulinid micronodules or a bioclastic wackestone were observed at the center of internal encrustations by coralline algae (Fig. 4).

From the taphonomic point of view, the rhodoliths showed random evidence of fragmentation and erosion at their surface, in contact with the *Orbulina* marls unit. Internally, the algal thalli did not show any extensive evidence of fragmentation, abrasion or bioerosion, although microscopic bioclastic fragments of heterogeneous origin (including coralline algae) were detected in the micritic infill of the rhodolith porosity.

4.2. The macrofossil association of Tornimparte

The blocks collected at Tornimparte ranged from bioclastic conglomerate to breccia (Fig. 5). The CT-scan images showed that the sampled deposits were chaotic, and fragments did not show grading or orientation (Fig. 6A-B, white arrows). The CT-scan data allowed to identify fossils as both entire specimens (Fig. 6B, red arrow), and fragments with broken and sharp edges, all cm-sized, together with phosphathic pebbles with rounded edges (Fig. 6A-B, white arrows) and evidence of glauconitization at their surface, detectable in thin section. The fossil paleocommunity included shark teeth, abundant bivalves, rare gastropods, encrusting cheilostome bryozoans on other biogenic substrates, echinoid fragments (mostly spines), solitary corals, rare brachiopods and benthic and planktonic foraminifers, including encrusting forms (Fig. 6C). Among mollusks, there were abundant fragments of oyster bivalves (Fig. 6C bottom), together with sparce specimens of pectinids. Gastropods were very scarce and were represented only by casts, including one specimen of a *Cerithium* sp., as well as a specimen belonging to the Calliostomatidae family (Fig. 6C, top). The solitary corals were mostly recrystallized, showing a trocoid to turbinate calix, with evidence of longitudinal, thin grooves on the external epitheca (Fig. 6C, center). The transverse outline ranges between circular to elliptical. Inside, two or three orders of septa could be distinguished, depending on the specimen, as well as a spongy columella (Fig. 6C, center). They belong to Caryophylliidae family.

The analysis of the thin sections allowed identifying the glauconitic wackestone with abundant planktonic foraminifera and phosphatic pebbles as the main components (Fig. 7). Fossils and pebbles were embedded in such material, showing variable abundance (Fig. 7). Interestingly, such wackestone (both glauconized and non) was easily identifiable also on CT-scan images, as it corresponded to the massive homogenous signal within the samples (Fig. 6A-B, green arrows).



Fig. 5. Field views from Tornimparte. A: in the Tornimparte outcrop, phosphatic levels occur in the uppermost part of the Miocene calcarenites and extend into the first meter of the overlying *Orbulina* marls. B: detail of the basal portion of the *Orbulina* marls. C: At the base, phosphatic lithoclasts up to 5 cm in diameter are dispersed within a phosphatized bioclastic matrix and associated with phosphatized fossils. D: In the upper part, phosphatic pebbles are dispersed within a marly planktonic wackestone matrix and are associated with phosphatized fossils and shark teeth.

5. Discussion

The compositional and taphonomic analyses carried out on the two phosphate levels investigated in this study provide insights into the environmental and oceanographic conditions controlling their formation.

5.1. The paleoenvironment of the Sirente Mt. rhodoliths

Rhodoliths are defined as nodules composed of >50% thickness coralline red algal thalli (Steneck, 1986; Foster, 2001; Basso et al., 2009) while the term macroids identifies an ample category of cm-sized biogenic nodules made of associations of metazoans or protozoans (Hottinger, 1983; Baarli et al., 2012). Biogenic nodules can show a complex composition, sometimes challenging a straightforward identification of macroids versus rhodoliths, based on dominant components (Reid and MacIntyre, 1988; Prager and Ginsburg, 1989; Bassi et al., 2012; Baarli et al., 2012; Bracchi et al., 2023). However, bryozoans and acervulinids at the rhodoliths core and intercalated with coralline thalli constitute always less than 50% of the total rhodolith thickness in our samples (Fig. 3). The term rhodolith, and not macroid, thus seems appropriate in our case (Hottinger, 1983; Vale et al., 2018; Bassi et al., 2024).

Contrary to early hypotheses about the relationship between rhodolith shape and hydrodynamics (Bosence, 1983), a growing body of evidence demonstrates that the spheroidal shape is by far the most frequently represented, both in modern rhodoliths beds and in the fossil record, and that no obvious environmental/paleoenvironmental interpretation can be obtained from rhodolith shape alone (Sañé et al., 2016; O'Connell et al., 2020; Bracchi et al., 2022; Bassi et al., 2024).

The observed rhodolith features and multispecific composition, their loose internal structure, the common porosity, and the diverse associated skeletal components, collectively identify the boxwork rhodoliths morphotype (Bosence, 1983; Basso, 1998; Villas-Boas et al., 2014; Basso et al., 2009; Adams et al., 2020; Olmstead and Andrus, 2024). Boxwork rhodoliths form under relatively low-intensity hydrodynamics and mechanical displacement. Their relative stability on the seafloor explains the fine sediment infilling, the typical occurrence of bioturbation, and the strong space competition resulting in alternating generations of encrusters and multispecific coralline builders. These complex algal concretions may record successive stages of discontinuous algal growth under fluctuating environmental conditions or following depth gradients controlled by sealevel changes (Basso and Tomaselli, 1994; Vale et al., 2018; Bracchi et al., 2019; Dulin et al., 2020). The two species of *Mesophyllum* identified in the Sirente rhodoliths were both described by Lemoine (1939) from the Tortonian outcrops of Saint Denis du Sig

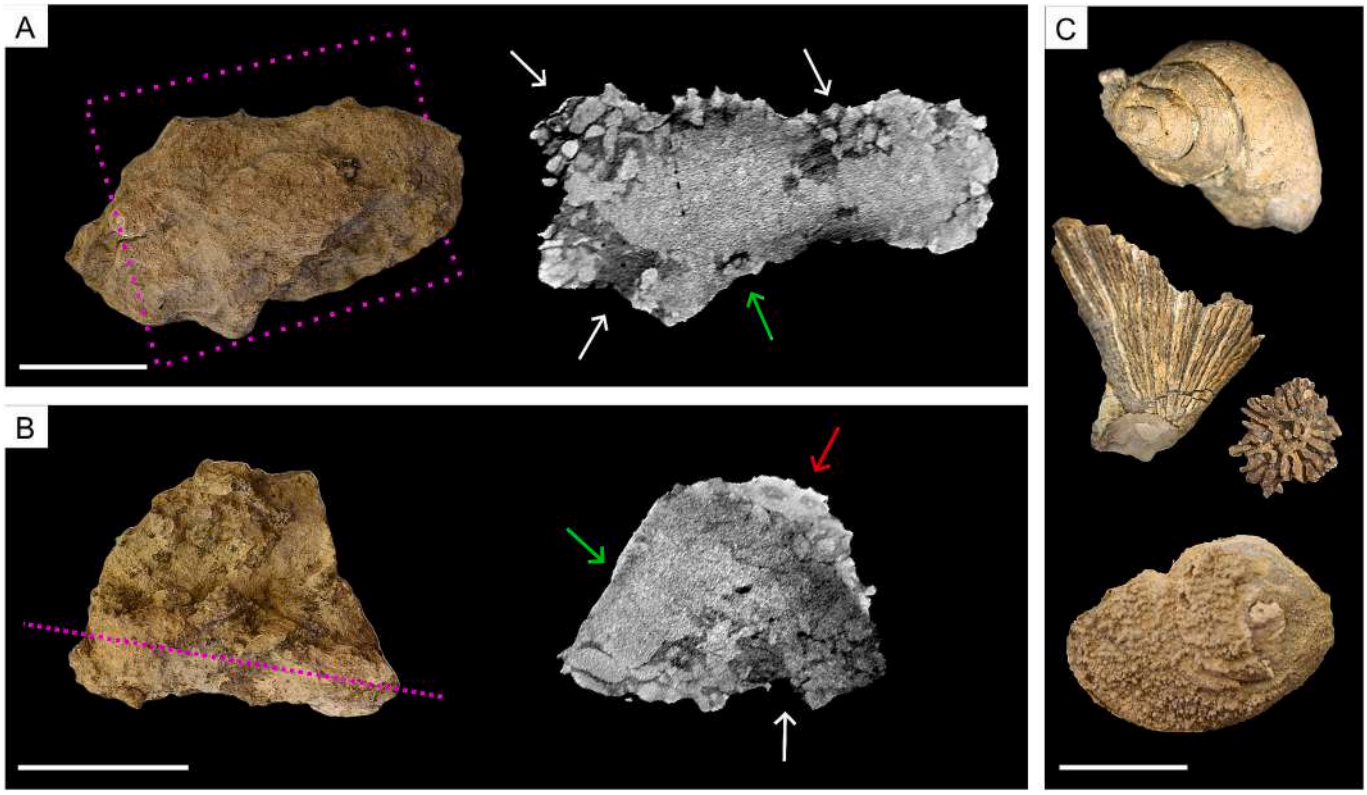


Fig. 6. Tornimparte samples and CT-scan images. A-B: two samples collected at Tornimparte on the left the samples, with the position of the slices shown by the dotted pink lines; on the right the corresponding CT-scan slice images. Phosphatized pebbles (white arrows) and fossils (red arrow) occur in both A and B. The green arrows indicate a massive homogeneous signal corresponding to wackestone containing abundant planktonic foraminifera showing signs of glauconitization. Scale bars in A and B = 3 cm. C: Examples of some fossils extracted from the Tornimparte samples. At the top: one specimen of oyster bivalve. In the center: on the left one specimen of solitary corals partially broken, showing a turbinate calix with longitudinal, thin grooves; on the right, one specimen of solitary corals cut in transversal section, with evident septa and spongy columella. At the bottom: one specimen belonging to the Calliostomatidae family. Scale bar = 1 cm. (For interpretation of the references to colour in this figure legend, the reader is referred to the web version of this article.)

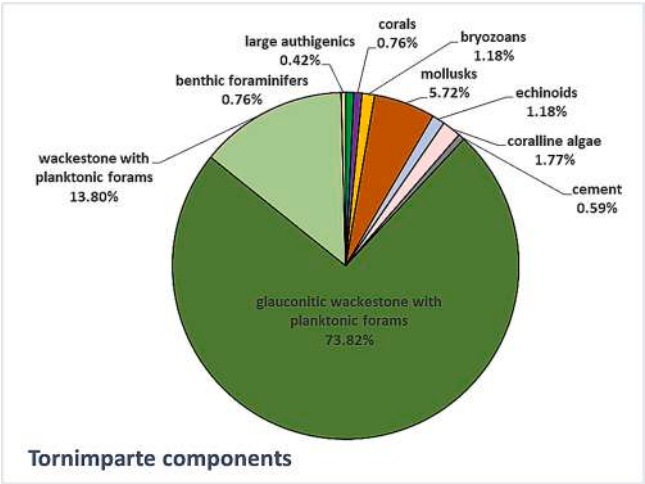


Fig. 7. Pie chart showing the mean contribution of the different categories to the composition of the Tornimparte samples. Data from point counting.

(Algeria) (Aguirre and Braga, 1998), and have been also identified in the Tortonian of southern Crete (Kroeger, 2007), pointing to a coherent biostratigraphic and paleoclimatic distribution.

Altogether, coralline algae show a direct relationship of growth and calcification with light and temperature, in all of the various environmental settings where they thrive. However, their positive response is observed up to a species-specific optimum level of light and temperature, beyond which metabolic performance deteriorates rapidly, leading to physiological stress or mortality (Fortes and Lüning, 1980; Hurd et al., 2014). This explains why corallines are distributed from the intertidal down to the deepest oligophotic zone, but coralline species distributions show much narrower ranges, depending also on climate zones and oceanographic controls, with many species preferring moderate or low light intensity (Adey et al., 1982; Iryu, 1992; Quaranta et al., 2012; Hurd et al., 2014; Coletti et al., 2018; Li et al., 2021).

In coral reefs, areas affected by seasonal upwelling are characterized by reduced coral abundance and biodiversity. An overall negative effect of upwelling on coralline abundance was reported by a meta-analysis of coral-reef benthic communities (Spring and Williams, 2023), although significant exceptions occur for some shallow-water species, such as *Porolithon* (Pulecio-Plaza et al., 2023). In vivo experiments have demonstrated that reduced light levels and high nutrient concentrations are detrimental to coralline algae, unless they are exposed to a moderate increase in pCO_2 (Johnson and Carpenter, 2018; Lewis et al., 2025). However, since coralline algae are less sensitive than stony corals to cooling, nutrient enrichment and turbidity increase driven by upwelling, this situation represents a competitive advantage for coralline development (Caragnano et al., 2017).

Encrusting bryozoans are a widespread and biodiverse group of colonial invertebrates. They are common cryptic dwellers and highly diverse components of mesophotic and oligophotic habitats, occurring in caves, and on the shadowed undersides of all types of solid substrates, including light-dependent builders such as corals and calcareous algae (Sanfilippo et al., 2011, 2015; Rosso et al., 2019; Giampaoletti et al., 2020). In the temperate circalittoral algal reefs of the present-day Mediterranean, the Coralligenous, they are typically the second most

important contributor to the growth of the calcareous framework (Basso et al., 2022; Donato et al., 2024). Bryozoans are also frequently recorded in multispecific, boxwork rhodoliths.

Their growth rates are quite variable, depending also on the colony morphology (erect, encrusting, etc.) and on the availability of food and space (Smith, 2007). Encrusting bryozoans show a linear growth rate ranging approximately between 1 and 10 mm y^{-1}, with a mean rate of about 3.2 mm y^{-1} (Smith, 2014). Growth rate in bryozoans is positively correlated with temperature (Lombardi et al., 2006; Smith, 2014), due to higher metabolic rates in warm waters (Smith and Lawton, 2010), and it is modulated by the availability of food (Buss, 1979).

Cold, nutrient-rich water from upwelling boosts phytoplankton growth, providing abundant food for filter-feeding bryozoans, and inducing water cooling and an increase of pCO_2 (Frazão et al., 2025). In the Baltic Sea, upwelling events of hypercapnic deep water masses to nearshore habitats are well-documented, inducing undersaturation of calcite and aragonite for periods of days to weeks (Lehmann et al., 2012). Experimental studies mimicking these upwelling events (about 1200 μatm) have demonstrated that bryozoan colonies raised under high CO_2 grow more quickly, although extreme hypercapnic waters (> 3000 μatm) are detrimental to bryozoan calcification (Saderne and Wahl, 2013; Swezey et al., 2017).

Encrusting foraminifera are quite common, although never dominant, in the Sirente Mt. rhodoliths (Fig. 3). They may act as habitat engineers and primary macroid builders (Perrin, 1992; Bassi et al., 2019; Bracchi et al., 2023). The development of acervulinids is interpreted as an indication of low competition for substrate occupation by other phyla of hard-substrate dwellers, which is one of the most critical factors controlling the biotic composition of sclerobiont communities (Reiss and Hottinger, 1984). Insufficient light for coralline algae is the most obvious competitive advantage for acervulinids, while disentangling the different competitive advantages of encrusting foraminifera vs. bryozoans is more challenging. It has been proposed that eutrophic deep waters, or upwelling, could sustain acervulinid development in their harsh and unfavorable competition with other sclerobionts (Dullo et al., 1990; Flamand et al., 2008; Schlagintweit et al., 2018; Brandano and Tomassetti, 2022). Although this is a plausible explanation, the lack of direct evidence supporting nutrients as drivers of successful acervulinids colonization suggests the need for further investigations (Bassi et al., 2024). Benthic foraminifera utilize a wide variety of food items, gathered by different feeding techniques (Lipps, 1983; Lee, 1980). As a general rule, non-symbiotic benthic foraminifera are mostly primary consumers or opportunists, consuming bacteria, diatoms and other microalgae together with organic-rich detritus that is captured by pseudopodia (Haynert et al., 2020; Courtial et al., 2025; Enge et al., 2014). Benthic foraminifera living within the photic zone commonly feed by grazing on algal cells and bacteria that cover the surface on which the foraminiferal cells move, while suspension feeding has been reported for some deep-sea species (Flach et al., 1998). In contrast, bryozoans are mostly primarily sessile, active suspension feeders, capturing suspended organic carbon sources such as phytoplankton (McKinney, 1990). From this point of view, oligotrophic dim-light waters with low suspended organic load should hamper both coralline algae (because of insufficient light) and bryozoan development (because of the lack of food) thereby providing a niche of competitive advantage for substrate occupation by the more opportunistic acervulinids (Perrin, 1992; Bosellini and Papazzoni, 2003; Bassi et al., 2024). Conversely, bryozoans are expected to easily outcompete coralline algae following an increase of nutrient and turbidity in deep oligophotic (circalittoral) environments, due to their faster growth rates (McCoy and Kamenos, 2015; Key, 2020). Recent investigations on living acervulinid macroids collected at 60–105 m of water depth offshore Kikai Island (Central Ryukyu Islands, southern Japan) revealed intergrown, subordinate thin hapalidialean coralline algae, together with other minor components as serpulids and bryozoans (Bassi et al., 2012, 2024). However, a significant difference is observed in the contribution of acervulinids, which represent a more conspicuous component inside the Japanese rhodoliths, in contrast to their subordinate role in the Sirente Mt. rhodoliths.

The analysed rhodolith composition revealed dominant *Mesophyllum* and subordinate *Lithothamnion*, scattered and rare sterile *Lithoporella* and *Titanoderma* sp., interposed with cheilostome bryozoans and with the occurrence of acervulinids and serpulids (Fig. 4). Some analogies can be searched in literature. Several analogies can be detected with the living rhodoliths collected at about 100 m depth on the deep Brazilian shelf (Peregrino Oil field, Tamega et al., 2014). The reported dominant coralline genus making up those Brazilian deep rhodoliths was *Mesophyllum,* associated with *Lithothamnion,* and the inner rhodoliths composition showed a trend of decreasing coralline algal contribution, accompanied by an increase of both bryozoans and *Acervulina* with increasing depth (from 100 to 106 m, Tamega et al., 2014). Also in the southeastern Brazil, *Mesophyllum* is the dominant genus identified in rhodolith-forming corallines at 90–100 m depths. Photosynthesis in this deep *Mesophyllum* species indicates strong acclimation to the dim conditions of deep waters and a very efficient absorption of low irradiance, explaining its dominance despite an extremely low growth rate (Figueiredo et al., 2012; Tamega et al., 2014). Very slow coralline growth in deep water was reported also by Littler et al. (1991) with values of 0.01–0.05 mm yr^{-1} at 61–91 m depth. High nutrient levels or sedimentation and related turbidity have been observed to promote bryozoan dominance over coralline algae around small bioclastic nuclei in the Brazilian shelf affected by the Amazon River plume (Vale et al., 2018).

Within a tropical/sub-tropical marine environment, the complete absence of corals and warm, shallow-water coralline algae and shallow benthic foraminifera, the dominance of thin thalli of Hapalidiales, mainly belonging to the genus *Mesophyllum,* and the recurrent encrustation by bryozoans, acervulinid, and, more sporadically, by annelids, suggest a deep shelf paleo-setting for the Sirente rhodoliths, coherent with a deep tropical oligophotic ramp, more likely in the range 70–90 m depth. Rhodoliths, as calcareous substrates exposed on the seafloor, are expected to undergo intense bioerosion, especially in deep waters under low nutrient inputs and low sedimentation rates (Bassi et al., 2013). In contrast, a decrease in bioturbation intensity with increasing depth was postulated by Checconi and Monaco (2008) based on an analysis of Middle Miocene rhodoliths of the Southern Apennines. The Sirente Mt. rhodoliths did not show any extensive internal bioturbation, which also supports a deep paleoenvironment of formation and drowning.

Based on the thickness of the algal-dominated versus bryozoan-dominated rhodolith layers, and in consideration of their plausible growth rates, it is possible to speculate about the approximate duration of the intervals favoring corallines and bryozoans, respectively. Given the extremely low growth rate of deep *Mesophyllum*, and the lack of thick encrustation or superposition among bryozoan colonies, it is reasonable to infer a fluctuation over several years, with possibly longer periods favorable to corallines than to bryozoans. Our data do not support the hypothesis of a simply seasonal pattern of upwelling, rather, they open the perspective of a multiannual frequency of more intense upwelling phases, similar to what presently occurs for some climate phenomena controlled by the combination of specific ocean and atmospheric conditions. Present-day upwelling occurrence exhibits interannual variability, as documented in the Peruvian (Chavez and Barber, 1987), Californian (Pennington and Chavez, 2000), and Benguela systems (Shannon, 1985). The timescale of this variability depends largely on fluctuations in wind stress. The Peruvian upwelling system represents a well-known example: during El Niño years, trade winds weaken or reverse, leading to a marked reduction in upwelling along the Peruvian coast (Gariboldi et al., 2023). Variations in wind intensity directly control interannual upwelling strength through Ekman transport (Bakun, 1990).

In the Taiwan system, upwelling intensifies during years of strengthened southwesterly winds (Hong et al., 2009). These wind variations are linked to anomalies in the East Asian Monsoon, which

develop following the onset of ENSO (El Niño) in the previous year. More generally, global warming may enhance coastal upwelling by increasing the land-sea thermal gradient, thus intensifying alongshore winds (Bakun, 1990). Indeed, this decadal variability in upwelling intensity is reflected in fluctuations in nutrient supply and, consequently, in productivity, water transparency, and light penetration (Kämpf and Chapman, 2017). The upwelling process has profound ecological consequence as it carries nutrient-rich subsurface water into the euphotic zone. Hence, the ecological effectiveness of the upwelling process critically depends on the properties of shelf bottom water. Nutrient concentrations in the sea generally increase with increasing water depth. Consequently, dynamic processes that move nutrient-rich seawater from the upper continental slope across the shelf break and onto the continental shelf can substantially enhance the biological productivity in an upwelling region (Kämpf and Chapman, 2017). In the outer ramp of the Tortonian Sirente Mt. platform, recurrent upwelling phases - also documented at a global scale in association with enhanced oceanic circulation and carbon-cycle perturbations (e.g., Carbon Maximum 7 of Holbourn et al., 2004) - likely exerted a primary control on ecosystem dynamics. These phases intermittently increased nutrient availability and turbidity, modulating light penetration and trophic structure. Such cyclical environmental forcing may have repeatedly shifted the competitive balance between coralline algae and suspension feeders. Periods of intensified upwelling would have promoted phytoplankton productivity and enhanced the food supply for bryozoans, favoring their episodic expansion. Conversely, intervals of reduced nutrient input and improved water transparency would have allowed the slow-growing but persistent, deep-water, *Mesophyllum*-dominated assemblages to regain ecological dominance. Rather than reflecting simple seasonal oscillations, the observed biotic alternations are more consistent with multiannual variability in upwelling intensity, comparable to that documented in modern wind-driven systems.

5.2. The paleoenvironment of the Tornimparte deposits

At Tornimparte, the identifiable elements of the sampled hardground, such as the gastropod *Cerithium* sp., as well as the cm-sized specimen belonging to the Calliostomatidae family, together with pectinids, ostreids and solitary corals, point to a potentially shallow, possibly infralittoral, marine paleocommunity. These fossils appear consistent from a paleoenvironmental point of view, and mixing with other fossil assemblages, representing different paleocommunities and habitats is ruled out. Concurrently, they are not compatible with the pelagic *Orbulina* marls unit in which these macrofossils were embedded and lithified.

Although diagenesis has obliterated the aragonite elements, meaning that gastropods and solitary corals are only present in recrystallized form or as casts, the fossil content shows taphonomic signatures that can provide insight into the sedimentation and depositional processes that affected them.

First, the fossils are centimeter-sized and, in the case of mollusks they are not representative of a natural population of invertebrates, in which a wide size distribution with a prevalence of small-sized specimens is expected. This potentially indicates the allochthonous nature of the assemblage. Furthermore, the most abundant elements, such as the remains of ostreid mollusks, often show signs of fragmentation with sharp angles. While fragmentation can occur after an animal's death and before its final burial in the sediment, size-selective fragmentation (in our case the uniform size of the specimens) implies an energy source capable of sorting and transporting fragments of a certain size and shape to a location different from their origin. Moreover, CT-scan analysis of the two blocks ruled out pebble orientation or grading, suggesting that this deposit should be interpreted as chaotic. Consequently, these findings suggest the transport and accumulation of allochthonous material (fossils) into unorganized deposits. It is therefore highly probable that the fragmentation is partly due to post-mortem transport, possibly occurring within an energetic shallow paleoenvironment, prior to erosion, subsequent further transport, and final burial in a deeper setting. A key factor controlling these erosional processes is the structure of the coastal upwelling system. In such environments, seawater is strongly density-stratified, with a well-developed and persistent pycnocline along which perturbations commonly propagate as internal waves (Walter et al., 2014, 2016). The phosphorite beds studied here are interpreted as the result of sediment accumulation driven by gravity flows, which were generated by turbulence associated with the breaking of internal waves on the seafloor of the outer ramp (Pomar et al., 2012). These gravity flows reworked the phosphatization zone where phosphatic crusts and laminae were forming, thereby eroding them and producing phosphatic lithoclasts. These clasts were subsequently transported and redeposited downslope, accumulating basinward (Brandano et al., 2020).

5.3. Autochthonous phosphate hardground vs. allochthonous phosphate-rich beds

Hardgrounds are widely documented in Miocene successions of the circum-Mediterranean region and are commonly interpreted as the result of the upwelling of nutrient-rich deep waters (Carannante, 1982; Pedley and Bennett, 1985; Simone and Carannante, 1988; Mutti and Bernoulli, 2003; Föllmi et al., 2008, 2015; Brandano et al., 2016, 2020). Coastal upwelling zones are typically characterized by sediments enriched in authigenic phosphorus.

A genetic model for the phosphatization of the Apennine platform seafloor was proposed by Mutti and Bernoulli (2003). According to these authors, cold, nutrient-rich upwelled waters warmed as they moved up the ramp, causing degassing and triggering early marine carbonate cementation. Simultaneously, upwelling enhanced surface-water productivity, and the resulting flux of organic matter to the seafloor supplied the phosphorus required for apatite mineralization. Phosphatization processes therefore record the influence of nutrient-rich waters along the margins of the oxygen minimum zone (Baturin, 1982).

In the Miocene Mediterranean, the widespread phosphate-rich intervals display diverse origins. An authigenic origin has been proposed for certain phosphate hardgrounds, such as those of the Menorca Islands (Brandano et al., 2016). In contrast, other platforms, including Apulia, Malta, and Hyblea, contain phosphate-rich sediments produced by multiple dynamic processes, resulting in autochthonous phosphatized layers associated with allochthonous phosphate-bearing deposits (Pedley and Bennett, 1985; Föllmi et al., 2008, 2015; Vescogni et al., 2018; Barbagallo et al., 2026). These processes involve sediment production followed by erosion, phosphatization and, locally, glauconitization, with subsequent erosional phases leading to the redeposition of allochthonous phosphate-rich beds (Föllmi et al., 2008; Föllmi, 2016).

6. Conclusions

- The Latium–Abruzzi Platform records both types of deposits: autochthonous phosphate hardgrounds and allochthonous phosphate-rich beds, occurring in different sectors of the carbonate platform and in distinct stratigraphic intervals, thus corresponding to separate events (Brandano et al., 2009, 2020).
- The Sirente Mt. phosphatic hardground is located in the northeastern sector of the Latium-Abruzzi domain, is late Tortonian in age, and represents the first case (autochthonous; Brandano et al., 2009), having developed on a fossil rhodolith bed. Coralline red algal thalli constitute >50% of the total boxwork rhodolith thickness, while encrusting bryozoans and acervulinids act as subordinate components. The complete absence of corals, warm, shallow-water coralline algae, and shallow benthic foraminifera - coupled with the dominance of thin-thalli *Mesophyllum* -indicates a deep tropical, oligophotic outer ramp paleo-setting, likely at depths of 70–90 m. The lack of extensive internal bioturbation further supports a deep,

low-energy depositional environment. The internal structure of the boxwork rhodoliths records a cyclical shift in builder dominance, driven by multiannual upwelling fluctuations: phases of intensified upwelling brought cold, nutrient-rich, hypercapnic waters, boosting phytoplankton productivity and turbidity, thus favoring the relatively rapid expansion of active suspension-feeding bryozoans; the intervening phases of slackened upwelling sustained conditions of reduced nutrient input, low phytoplankton productivity and improved water transparency, allowing the slow-growing, deep-water *Mesophyllum* assemblages to regain ecological dominance. The Sirente Mt. rhodoliths captured the ecological imprint of long-term oceanographic fluctuations, expressed through subtle yet recurrent reorganizations of the benthic community. Overall, the integration of sedimentological, compositional, and taphonomic evidence supports a model in which outer-ramp rhodolith development was tightly coupled to upwelling-driven nutrient dynamics, providing a refined paleoceanographic perspective on Tortonian Mediterranean shelf environments.

- The Tornimparte phosphate-rich deposits, located in the northern area of the Latium-Abruzzi platform, are early Tortonian in age, and exemplify the second situation (allochthonous). At the Tornimparte outcrop, the phosphatic deposits are characterized by pronounced erosional features, including abundant reworked phosphatized and non-phosphatized fossils, as well as hardground lithoclasts displaying varying degrees of phosphatization (Brandano et al., 2020). Phosphate precipitation occurred within sediments accumulating in the aphotic zone of the outer ramp, under the influence of coastal upwelling. In this setting, phosphatic hardgrounds formed through the early diagenetic precipitation of carbonate fluorapatite within suboxic, organic-rich sediments (Brandano et al., 2020). The macrofossil assemblage (including *Cerithium* sp., Calliostomatidae, pectinids, ostreids, and solitary corals) indicates a shallow, infralittoral marine paleocommunity. This fauna is bathymetrically incompatible with the deeper pelagic *Orbulina* marls in which they were buried. The sorting of centimeter-sized mollusk remains, size-selective fragmentation of ostreids, and the lack of pebble orientation or grading (confirmed via CT-scan) indicate a chaotic, allochthonous deposit shaped by a high-energy source. Reworked shallow-water fossils and phosphatized hardground lithoclasts were transported downslope via gravity flows. We suggest that these flows were triggered by turbulent internal waves breaking along the pycnocline within a strongly stratified, upwelling coastal system.
- The comparison between the autochthonous rhodolith-bearing hardground of Sirente Mt. and the allochthonous phosphate-rich deposits of Tornimparte highlights how different fossil assemblages, taphonomic and sedimentological processes can record the overarching drivers of sediment starvation under the effect of nutrient-rich waters, providing a comprehensive framework for reconstructing the complex upwelling dynamics of the Tortonian Mediterranean platform.

CRediT authorship contribution statement

Daniela Basso: Writing – review & editing, Writing – original draft, Visualization, Supervision, Resources, Methodology, Investigation, Formal analysis, Data curation, Conceptualization. **Valentina Alice Bracchi:** Writing – review & editing, Writing – original draft, Visualization, Methodology, Investigation, Formal analysis, Data curation, Conceptualization. **Irene Cornacchia:** Writing – review & editing, Writing – original draft, Visualization, Investigation, Formal analysis. **Alessandro Mancini:** Writing – review & editing, Visualization, Investigation, Formal analysis. **Marco Brandano:** Writing – review & editing, Writing – original draft, Visualization, Supervision, Resources, Methodology, Investigation, Formal analysis, Conceptualization.

Declaration of competing interest

The authors declare that they have no known competing financial interests or personal relationships that could have appeared to influence the work reported in this paper.

Acknowledgements

We are grateful to two anonymous reviewers and to the Editor, Lucia Angiolini, for their constructive comments and suggestions, that significantly improved the first draft of the manuscript. We acknowledge the technical support of Elena de Ponti, Nuclear Medicine Department, S. Gerardo Hospital, Monza, and Fondazione Tecnomed, University of Milano-Bicocca, for the use of the TC scanner.

Data availability

Data are avilable upon request

References

Adams, L.A., Maneveldt, G.W., Green, A., Karenyi, N., Parker, D., Samaai, T., Kerwath, S., 2020. Rhodolith bed discovered off the South African coast. Diversity 12 (4), 125. https://doi.org/10.3390/d12040125.

Adey, W.H., Townsend, R.A., Boykins, W.T., 1982. The crustose coralline algae (Rhodophyta: Corallinaceae) of the Hawaiian Islands. Smithson. Contrib. Mar. Sci. 15, 1–74. https://doi.org/10.5479/si.01960768.15.1.

Aguirre, J., Braga, J.C., 1998. Redescription of Lemoine's (1939) types of coralline algal species from Algeria. Palaeontology 41, 489–507.

Baarli, B.G., Santos, A., Da Silva, C.M., Ledesma-Vázquez, J., Mayoral, E., Cachao, M., Johnson, M.E., 2012. Diverse macroids and rhodoliths from the upper Pleistocene of Baja California Sur, Mexico. J. Coast. Res. 28, 296–305.

Bakun, A., 1990. Global climate change and intensification of coastal ocean upwelling. Science 247 (4939), 198–201. https://doi.org/10.1126/science.247.4939.198.

Barbagallo, V., Cornacchia, I., Commis, L., Distefano, S., Mancini, A., Cormaci, A., Brandano, M., Maniscalco, R., Catalano, S., Di Stefano, A., 2026. Integrated stratigraphy of Oligocene-Miocene phosphate-bearing layers in the frame of the Central Mediterranean paleoceanography: insights from the western Hyblean Plateau sedimentary record (SE Sicily, Italy). Palaeogeogr. Palaeoclimatol. Palaeoecol. 690, 113717. https://doi.org/10.1016/j.palaeo.2026.113717.

Bassi, D., Humblet, M., Iryu, Y., 2012. Recent ichnocoenosis in deep water macroids, Ryukyu Islands, Japan. Palaios 26 (4), 232–238. https://doi.org/10.2110/palo.2010.p10-093r.

Bassi, D., Iryu, Y., Braga, J.C., Takayanagi, H., Tsuji, Y., 2013. Bathymetric distribution of ichnocoenoses from recent subtropical algal nodules off Fraser Island, eastern Australia. Palaeogeogr. Palaeoclimatol. Palaeoecol. 369, 58–66. https://doi.org/10.1016/j.palaeo.2012.10.003.

Bassi, D., Iryu, Y., Humblet, M., Matsuda, H., Machiyama, H., Sasaki, K., Inoue, T., 2019. Deep-water macroid beds of the Ryukyu Islands, Japan: encrusting acervulinids as ecosystem engineers. J. Coast. Res. 35, 463–466. https://doi.org/10.2112/JCOASTRES-D-18-00049.1.

Bassi, D., Braga, J.C., Asami, R., Goto, K., Szidat, S., Takayanagi, H., Iryu, Y., 2024. Paleoenvironmental significance of growth story of long-living deep-water acervulinid macroids from Kikai-jima shelf, Central Ryukyu Islands. Palaeogeogr. Palaeoclimatol. Palaeoecol. 647, 112254. https://doi.org/10.1016/j.palaeo.2024.112254.

Basso, D., 1998. Deep rhodolith distribution in the Pontian Islands, Italy: a model for the paleoecology of a temperate sea. Palaeogeogr. Palaeoclimatol. Palaeoecol. 137, 173–187. https://doi.org/10.1016/S0031-0182(97)00099-0.

Basso, D., Tomaselli, V., 1994. Paleoecological potentiality of rhodoliths: a Mediterranean case history. In: Matteucci, R., Carboni, M.G., Pignatti, J.S. (Eds.), Studies on Ecology and Paleoecology of Benthic Communities, 33. Boll. Soc. Paleont. It, pp. 17–28.

Basso, D., Favega, P., Piazza, M., Vannucci, G., 1998. Biostratigraphic, paleobiogeographic and paleoecological implications in the taxonomic review of Corallinaceae. Rend. Lincei Sci. Fis. Nat. 9 (3), 201–211.

Basso, D., Nalin, R., Nelson, C.S., 2009. Shallow-water *Sporolithon* rhodoliths from North Island (New Zealand). Palaios 24, 92–103. https://doi.org/10.2110/palo.2008.p08-048r.

Basso, D., Bracchi, V.A., Bazzicalupo, P., Martini, M., Maspero, F., Bavestrello, G., 2022. Living coralligenous as geo-historical structure built by coralline algae. Front. Earth Sci. 10, 961632. https://doi.org/10.3389/feart.2022.961632.

Baturin, G.N., 1982. Phosphorites on the sea floor. In: Developments in Sedimentology, 33. Elsevier (eBook ISBN: 9780080869476).

Bosellini, F.R., Papazzoni, C.A., 2003. Palaeoecological significance of coral–encrusting foraminiferan associations: a case–study from the Upper Eocene of northern Italy. Acta Palaeontol. Pol. 48, 279–292.

Bosence, D.W., 1983. The occurrence and ecology of recent rhodoliths - a review. In: Peryt, T.M. (Ed.), Coated Grains. Springer-Verlag, Berlin, pp. 225–242.

Bracchi, V., Angeletti, L., Marchese, F., Taviani, M., Cardone, F., Hajdas, I., Grande, V., Prampolini, M., Caragnano, A., Corselli, C., Basso, D., 2019. A resilient deep-water rhodolith bed off the Egadi Archipelago (Mediterranean Sea) and its actuopaleontological significance. Alp. Mediterr. Quat. 32, 131–150. https://doi.org/10.26382/AMQ.2019.09.

Bracchi, V.A., Caronni, S., Meroni, A.N., Burguett, E.G., Atzori, F., Cadoni, N., Basso, D., 2022. Morphostructural characterization of the heterogeneous rhodolith bed at the Marine Protected Area "Capo Carbonara" (Italy) and hydrodynamics. Diversity 14, 51. https://doi.org/10.3390/d14010051.

Bracchi, V.A., Purkis, S.J., Marchese, F., Nolan, M.K.B., Terraneo, T.I., Vimercati, S., Chimienti, G., Rodrigue, M., Eweida, A., Benzoni, F., 2023. Mesophotic foraminiferal-algal nodules play a role in the Red Sea carbonate budget. Commun. Earth Environ. 4, 288. https://doi.org/10.1038/s43247-023-00944-w.

Braga, J.C., 2003. Application of botanical taxonomy to fossil coralline algae (Corallinales, Rhodophyta). Acta Micropaleontol. Sin. 20, 47.

Brandano, M., 2002. La Formazione dei "Calcari a Briozoi e Litotamni" nell'area di Tagliacozzo (Appennino Centrale) e considerazioni paleoambientali sulle facies rodalgali. Boll. Soc. Geol. Ital. 121, 179–186.

Brandano, M., 2003. Tropical/subtropical inner ramp facies in lower Miocene" Calcari a Briozoi e Litotamni" of the Monte Lungo area (Cassino Plain, Central Apennines, Italy). Boll. Soc. Geol. Ital. 122, 85–98.

Brandano, M., 2017. Unravelling the origin of a Paleogene unconformity in the Latium-Abruzzi carbonate succession: a shaved platform. Palaeogeogr. Palaeoclimatol. Palaeoecol. 485, 687–696. https://doi.org/10.1016/j.palaeo.2017.07.025.

Brandano, M., Corda, L., 2002. Nutrients, sea level and tectonics: constrains for the facies architecture of a Miocene carbonate ramp in central Italy. Terra Nova 14, 257–262. https://doi.org/10.1046/j.1365-3121.2000.00419.x.

Brandano, M., Tomassetti, L., 2022. MECO and Alpine orogenesis: constraints for facies evolution of the Bartonian nummulitic and *Solenomeris* limestone in the Argentina Valley (Ligurian Alps). Sedimentology 69, 24–46. https://doi.org/10.1111/sed.12829.

Brandano, M., Mateu-Vicens, G., Gianfagna, A., Corda, L., Billi, A., Quaresima, S., Simonetti, A., 2009. Hardground development and drowning of a Miocene carbonate ramp (Latium-Abruzzi): from tectonic to paleoclimate. J. Mediterr. Earth Sci. 1, 47–56. https://doi.org/10.3304/JMES.2009.004.

Brandano, M., Brilli, M., Corda, L., Lustrino, M., 2010. Miocene C-isotope signature from the central Apennine successions (Italy): monterey vs. regional controlling factors. Terra Nova 22, 125–130. https://doi.org/10.1111/j.1365-3121.2010.00925.x.

Brandano, M., Westphal, H., Mateu-Vicens, G., Preto, N., Obrador, A., 2016. Ancient upwelling record in a phosphate hardground (Tortonian of Menorca, Balearic Islands, Spain). Mar. Pet. Geol. 78, 593–605. https://doi.org/10.1016/j.marpetgeo.2016.07.017.

Brandano, M., Cornacchia, I., Raffi, I., Tomassetti, L., Agostini, S., 2017. The Monterey Event within the Central Mediterranean area: the shallow-water record. Sedimentology 64, 286–310. https://doi.org/10.1111/sed.12348.

Brandano, M., Ronca, S., Di Bella, L., 2020. Erosion of Tortonian phosphatic intervals in upwelling zones: the role of internal waves. Palaeogeogr. Palaeoclimatol. Palaeoecol. 537, 109405. https://doi.org/10.1016/j.palaeo.2019.109405.

Brigaud, B., Vincent, B., Durlet, C., Deconinck, J.F., Jobard, E., Pickard, N., Yven, B., Landrein, P., 2014. Characterization and origin of permeability–porosity heterogeneity in shallow-marine carbonates: from core scale to 3D reservoir dimension (Middle Jurassic, Paris Basin, France). Mar. Pet. Geol. 57, 631–651. https://doi.org/10.1016/j.marpetgeo.2014.07.004.

Buss, L., 1979. Bryozoan overgrowth interactions—the interdependence of competition for space and food. Nature 281, 475–477. https://doi.org/10.1038/281475a0.

Caragnano, A., Basso, D., Storz, D., Jacob, D.E., Ragazzola, F., Benzoni, F., Dutrieux, E., 2017. Elemental variability in the coralline alga *Lithophyllum yemenense* as an archive of past climate in the Gulf of Aden (NW Indian Ocean). J. Phycol. 53, 381–395. https://doi.org/10.1111/jpy.12509.

Carannante, G., 1982. Modello deposizionale e diagenetico di un livello fosfatico nel Miocene carbonatico dell'Appennino campano. Rend. Soc. Geol. Ital. 5, 15–20.

Carannante, G., Esteban, M., Milliman, J., Simone, L., 1988. Carbonate facies as paleolatitude indicators: problems and limitations. Sediment. Geol. 60, 333–346.

Chavez, F.P., Barber, R.T., 1987. An estimate of new production in the equatorial Pacific. Deep-Sea Res. I Oceanogr. Res. Pap. 34, 1229–1243. https://doi.org/10.1016/0198-0149(87)90073-2.

Checconi, A., Monaco, P., 2008. Trace fossil assemblages in rhodoliths from the Middle Miocene of Mt. Camposauro (Longano formation, southern Apennines, Italy). Studi Trent. Sci. Nat., Acta Geol. 83, 165–176.

Chen, C., Zhong, H., Wang, X., Ning, M., Wang, X., Wang, H., Tang, R., Hou, M., 2025. Recent marine carbonate hardgrounds at Abu Dhabi: towards a better understanding of 'hidden hardgrounds' in the geological past. Front. Mar. Sci. 12, 1552576. https://doi.org/10.3389/fmars.2025.1552576.

Christ, N., Immenhauser, A., Wood, R.A., Darwich, K., Niedermayr, A., 2015. Petrography and environmental controls on the formation of Phanerozoic marine carbonate hardgrounds. Earth Sci. Rev. 151, 176–226. https://doi.org/10.1016/j.earscirev.2015.10.002.

Cipollari, P., Cosentino, D., 1995. Miocene unconformities in the Central Apennines: geodynamic significance and sedimentary basin evolution. Tectonophysics 252, 375–389. https://doi.org/10.1016/0040-1951(95)00088-7.

Civitelli, G., Brandano, M., 2005. Atlante delle litofacies e modello deposizionale dei Calcari a Briozoi e Litotamni nella Piattaforma carbonatica laziale-abruzzese. Boll. Soc. Geol. Ital. 124, 611.

Coletti, G., Basso, D., Corselli, C., 2018. Coralline algae as depth indicators in the Sommières Basin (early Miocene, Southern France). Geobios 51, 15–30. https://doi.org/10.1016/j.geobios.2017.12.002.

Corda, L., Brandano, M., 2003. Aphotic zone carbonate production on a Miocene ramp, Central Apennines, Italy. Sediment. Geol. 161, 55–70. https://doi.org/10.1016/S0037-0738(02)00395-0.

Cornacchia, I., Brandano, M., Agostini, S., Munnecke, A., 2022. Neodymium isotopes of central Mediterranean phosphatic hardgrounds reveal Miocene paleoceanography. Geology 50, 1023–1027. https://doi.org/10.1130/G50118.1.

Corselli, C., Basso, D., Garzanti, E., 1994. Paleobiological and sedimentological evidence of Pleistocene/Holocene hiatuses and ironstone formation at the Pontian islands shelfbreak (Italy). Mar. Geol. 117, 317–328. https://doi.org/10.1016/0025-3227(94)90023-X.

Cosentino, D., Carboni, M.G., Cipollari, P., Di Bella, L., Florindo, F., Laurenzi, A.M., Sagnotti, L., 1997. Integrated stratigraphy of the Tortonian/Messinian boundary: the Pietrasecca composite section (central Apennines, Italy). Eclogae Geol. Helv. 90, 229–244.

Courtial, J., Lothier, J., Cukier, C., Limami, A.M., Geslin, E., 2025. Metabolic adaptations of benthic forams: foraminiferal species adaptations to intertidal mudflat assessed by a metabolic approach. J. Eukaryot. Microbiol. 72, e70051. https://doi.org/10.1111/jeu.70051.

Damiani, A.V., Chiocchini, M., Colacicchi, R., Mariotti, G., Parotto, M., Passeri, L., Praturlon, A., 1992. Elementi litostratigrafici per una sintesi delle facies carbonatiche meso-cenozoiche dell'Appennino centrale. Studi Geol. Camerti 2, 187–213. https://doi.org/10.15165/studgeocam-1410.

Doglioni, C., 1991. A proposal for the kinematic modelling of W-dipping subductions-possible applications to the Tyrrhenian-Apennines system. Terra Nova 3, 423–434.

Donato, G., Sanfilippo, R., Basso, D., Bazzicalupo, P., Bertolino, M., Bracchi, V.A., Rosso, A., 2024. Biodiversity associated with a coralligenous build-up off Sicily (Ionian Sea). Reg. Stud. Mar. Sci. 80, 103868. https://doi.org/10.1016/j.rsma.2024.103868.

Dulin, T., Avnaim-Katav, S., Sisma-Ventura, G., Bialik, O.M., Angel, D.L., 2020. Rhodolith beds along the southeastern Mediterranean inner shelf: implications for past depositional environments. J. Mar. Syst. 201, 103241. https://doi.org/10.1016/j.jmarsys.2019.103241.

Dullo, W.C., Moussavian, E., Brachert, T.C., 1990. The foralgal crust facies of the deeper fore reefs in the Red Sea: a deep diving survey by submersible. Geobios 23, 261–281. https://doi.org/10.1016/0016-6995(90)80001-V.

Enge, A.J., Witte, U., Kucera, M., Heinz, P., 2014. Uptake of phytodetritus by benthic foraminifera under oxygen depletion at the Indian margin (Arabian Sea). Biogeosciences 11, 2017–2026. https://doi.org/10.5194/bg-11-2017-2026.

Figueiredo, M.A.O., Coutinho, R., Villas-Boas, A.B., Tâmega, F.T.S., Mariath, R., 2012. Deep-water rhodolith productivity and growth in the southwestern Atlantic. J. Appl. Phycol. 24, 487–493. https://doi.org/10.1007/S10811-012-9802-8.

Flach, E., Lavaleye, M., de Stigter, H., Thomsen, L., 1998. Feeding types of the benthic community and particle transport across the slope of the N.W. European continental margin (Goban Spur). Prog. Oceanogr. 42, 209–231. https://doi.org/10.1016/S0079-6611(98)00035-4.

Flamand, B., Cabioch, G., Payri, C., Pelletier, B., 2008. Nature and biological composition of the New Caledonian outer barrier reef slopes. Mar. Geol. 250, 157–179. https://doi.org/10.1016/j.margeo.2007.12.002.

Flügel, E., 2010. Microfacies of Carbonate Rocks - Analysis, Interpretation and Application. Springer.

Föllmi, K.B., 1996. The phosphorus cycle, phosphogenesis and marine phosphate-rich sediments. Earth Sci. Rev. 40, 55–124. https://doi.org/10.1016/0012-8252(95)00039-6.

Föllmi, K.B., 2016. Sedimentary condensation. Earth-Sci. Rev. 152, 143–180. https://doi.org/10.1016/j.earscirev.2015.11.016.

Föllmi, K.B., Weissert, H., Bisping, M., Funk, H., 1994. Phosphogenesis, carbon-isotope stratigraphy, and carbonate-platform evolution along the Lower Cretaceous northern Tethyan margin. Geol. Soc. Am. Bull. 106, 729–746.

Föllmi, K.B., Gertsch, B., Renevey, J.P., De Kaenel, E., Stille, P., 2008. Stratigraphy and sedimentology of phosphate-rich sediments in Malta and south-eastern Sicily (latest Oligocene to early Late Miocene). Sedimentology 55, 1029–1051. https://doi.org/10.1111/j.1365-3091.2007.00935.x.

Föllmi, K.B., Bôle, M., Jammet, N., Froidevaux, P., Godet, A., Bodin, S., Adatte, T., Matera, V., Fleitmann, D., Spangenberg, J.E., 2011. Bridging the Faraoni and Selli oceanic anoxic events: short and repetitive dys-and anaerobic episodes during the late Hauterivian to early Aptian in the central Tethys. Clim. Past Discuss. 7. https://doi.org/10.5194/cp-8-171-2012.

Föllmi, K.B., Hofmann, H., Chiaradia, M., de Kaenel, E., Frijia, G., Parente, M., 2015. Miocene phosphate-rich sediments in Salento (southern Italy). Sediment. Geol. 327, 55–71. https://doi.org/10.1016/j.sedgeo.2015.07.009.

Fortes, M.D., Lüning, K., 1980. Growth rates of North Sea macroalgae in relation to temperature, irradiance and photoperiod. Helgol. Meeresunters. 34, 15–29.

Foster, M.S., 2001. Rhodoliths: between rocks and soft places. J. Phycol. 37, 659–667. https://doi.org/10.1046/j.1529-8817.2001.00195.x.

Frazão, H.C., Send, U., Sutton, A.J., Ohman, M.D., Lankhorst, M., Martz, T.R., Sevadjian, J., 2025. Open ocean versus upwelling regimes: air-sea CO_2 fluxes and pCO_2 inter-annual variability in the Southern California Current System. J. Geophys. Res. Oceans 130, e2024JC022126. https://doi.org/10.1029/2024JC022126.

Gariboldi, K., Pike, J., Malinverno, E., Di Celma, C., Gioncada, A., Bianucci, G., 2023. Paleoceanographic implications of diatom seasonal laminations in the Upper Miocene Pisco Formation (Ica Desert, Peru) and their clues on the development of the Pisco Fossil-Lagerstätte. Paleoceanogr. Paleoclimatol. 38, e2022PA004566. https://doi.org/10.1029/2022PA004566.

Garrison, R.E., Luternauer, J.L., Grill, E.V., MacDonald, R.D., Murray, J.W., 1969. Early diagenetic cementation of recent sands, Fraser River delta, British Columbia. Sedimentology 12, 27–46.

Giampaoletti, J., Cardone, F., Corriero, G., Gravina, M.F., Nicoletti, L., 2020. Sharing and distinction in biodiversity and ecological role of bryozoans in Mediterranean mesophotic bioconstructions. Front. Mar. Sci. 7, 581292. https://doi.org/10.3389/fmars.2020.581292.

Glenn, C.R., Arthur, M.A., 1988. Early diagenesis models for phosphate precipitation and settings of authigenic phosphate formation. Mar. Geol. 81, 57–79. https://doi.org/10.1016/0025-3227(88)90031-5.

Godet, A., Föllmi, K.B., Spangenberg, J.E., Bodin, S., Vermeulen, J., Adatte, T., Bonvallet, L., Arnaud, H., 2013. Deciphering the message of Early Cretaceous drowning surfaces from the Helvetic Alps: what can be learnt from platform to basin correlations? Sedimentology 60, 152–173. https://doi.org/10.1111/sed.12008.

Guiry, M.D., Guiry, G.M., 2026. AlgaeBase. World-wide Electronic Publication, University of Galway. https://www.algaebase.org (searched on 16th January 2026).

Haynert, K., Gluderer, F., Pollierer, M.M., Scheu, S., Wehrmann, A., 2020. Food Spectrum and Habitat-specific diets of benthic foraminifera from the Wadden Sea – a Fatty Acid Biomarker Approach. Front. Mar. Sci. 7, 510288. https://doi.org/10.3389/fmars.2020.510288.

Holbourn, A., Kuhnt, W., Simo, J.T., Li, Q., 2004. Middle Miocene isotope stratigraphy and paleoceanographic evolution of the northwest and southwest Australian margins (Wombat Plateau and Great Australian Bight). Palaeogeogr. Palaeoclimatol. Palaeoecol. 208, 1–22. https://doi.org/10.1016/j.palaeo.2004.02.003.

Hong, H., Caiyun, Z., Shaoling, S., Bangqin, H., Yonghong, L., Xueding, L., Shimin, Z., 2009. Interannual variability of summer coastal upwelling in the Taiwan Strait. Cont. Shelf Res. 29, 479–484. https://doi.org/10.1016/j.csr.2008.11.007.

Hottinger, L., 1983. Neritic macroid genesis, an ecological approach. In: Peryt, T.M. (Ed.), Coated Grains. Springer, Berlin Heidelberg, pp. 38–55.

Hrabovský, J., Basso, D., Doláková, N., 2016. Diagnostic characters in fossil coralline algae (Corallinophycidae: Rhodophyta) from the Miocene of southern Moravia (Carpathian Foredeep, Czech Republic). J. Syst. Palaeontol. 14, 499–525. https://doi.org/10.1080/14772019.2015.1071501.

Hurd, C.L., Harrison, P.J., Bischof, K., Lobban, C.S., 2014. Seaweed Ecology and Physiology. Cambridge University Press (ISBN: 9781139192637).

Iryu, Y., 1992. Fossil nonarticulated coralline algae as depth indicators for the Ryukyu Group. Trans. Proc. Palaeont. Soc. Jpn. 167, 1165–1179.

Johnson, M.D., Carpenter, R.C., 2018. Nitrogen enrichment offsets direct negative effects of ocean acidification on a reef-building crustose coralline alga. Biol. Lett. 14, 20180371. https://doi.org/10.1098/rsbl.2018.0371.

Kämpf, J., Chapman, P., 2017. Upwelling Systems of the World. https://doi.org/10.1007/978-3-319-42524-5_231.

Kennedy, W.J., Garrison, R.E., 1975. Morphology and genesis of nodular chalks and hardgrounds in the Upper Cretaceous of southern England. Sedimentology 22, 311–386. https://doi.org/10.1111/j.1365-3091.1975.tb01637.x.

Key, M., 2020. Growth geometry and measurement of growth rates in marine bryozoans: a review. In: Bryozoan Stud. 2019..

Kroeger, K.F., 2007. Upper Miocene coralline red algal associations of central Crete (Greece): taxonomy and palaeoenvironmental implications. Neues Jahrb. Geol. Paläont. Ab. Band 244, 143–171. https://doi.org/10.1127/0077-7749/2007/0244-0143.

Lee, J.J., 1980. Nutrition and physiology of the foraminifera. In: Levandowsky, M., Hutner, S.H. (Eds.), Biochemistry and Physiology of Protozoa, vol. 3. Academic Press, Inc, New York, Usa; London, England.

Lehmann, A., Myrberg, K., Höflich, K., 2012. A statistical approach to coastal upwelling in the Baltic Sea based on the analysis of satellite data for 1990–2009. Oceanologia 54 (3), 369–393.

Lemoine, M., 1939. Algues calcaires fossiles de l'Algérie. Matériaux pour la Carte Géologique de L'Algérie. 1re Sér. Paléontol. 9, 1–128.

Lewis, B., Bender-Champ, D., Dove, S., Diaz-Pulido, G., 2025. CO_2 Fertilisation counteracts the negative effect of poor water quality on the growth and photosynthesis of a Great Barrier Reef coralline alga. Aquat. Conserv. Mar. Freshwat. Ecosyst. 35, e70042. https://doi.org/10.1002/aqc.70042.

Li, Y., Yu, K., Bian, L., Fan, T., Wang, R., Jiang, W., Yang, Y., 2021. Paleo-water depth variations since the Pliocene as recorded by coralline algae in the South China Sea. Palaeogeogr. Palaeoclimatol. Palaeoecol. 562, 110107. https://doi.org/10.1016/j.palaeo.2020.110107.

Lipps, J.H., 1983. Biotic interactions in benthic foraminifera. In: Tevesz, M.J., McCall, P.L. (Eds.), Biotic Interactions in Recent and Fossil Benthic Communities. Plenum, New York, pp. 331–376.

Littler, M.M., Littler, D.S., Hanisak, M.D., 1991. Deep-water rhodolith distribution, productivity, and growth history at sites of formation and subsequent degradation. J. Exp. Mar. Biol. Ecol. 150, 163–182.

Lombardi, C., Cocito, S., Occhipinti-Ambrogi, A., Hiscock, K., 2006. The influence of seawater temperature on zooid size and growth rate in *Pentapora fascialis* (Bryozoa: Cheilostomata). Mar. Biol. 149, 1103–1109. https://doi.org/10.1007/s00227-006-0295-3.

Loutit, T.S., Hardenbol, J., Vail, P.R., Baum, G.R., 1988. Condensed sections: the key to age determination and correlation of continental margin sequences. Sea-level changes—an integrated approach. In: Wilgus, C.K., Hastings, B.S., Posamentier, H., Wagoner, J.V., Ross, C.A., Kendall, C.G.St.C. (Eds.), Spec. Publ. Soc. Econ. Paleontol. Mineral., 42, pp. 184–213. https://doi.org/10.2110/pec.88.01.0183.

McCoy, S.J., Kamenos, N.A., 2015. Coralline algae (Rhodophyta) in a changing world: integrating ecological, physiological, and geochemical responses to global change. J. Phycol. 51, 6–24. https://doi.org/10.1111/jpy.12262.

McKinney, F.K., 1990. Feeding and associated colony morphology in marine bryozoans. Rev. Aquat. Sci. 2, 55–80.

Mutti, M., Bernoulli, D., 2003. Early marine lithification and hardground development on a Miocene ramp (Maiella, Italy): key surfaces to track changes in trophic resources in nontropical carbonate settings. J. Sediment. Res. 73, 296–308.

Nebelsick, J.H., Bassi, D., Lempp, J., 2013. Tracking paleoenvironmental changes in coralline algal-dominated carbonates of the Lower Oligocene Calcareniti di Castelgomberto formation (Monti Berici, Italy). Facies 59, 133–148. https://doi.org/10.1007/s10347-012-0349-6.

Nelson, C.S., 1988. An introductory perspective on non-tropical shelf carbonates. Sediment. Geol. 60, 3–12.

O'Connell, L.G., James, N.P., Harvey, A.S., Luick, J., Bone, Y., Shepherd, S.A., 2020. Reevaluation of the inferred relationship between living rhodolith morphologies, their movement, and water energy: Implications for interpreting paleoceanographic conditions. Palaios 35, 543–556. https://doi.org/10.2110/palo.2019.101.

Olmstead, S.A., Andrus, C.F.T., 2024. Growth characterization of mesophotic rhodoliths in the northern Gulf of Mexico using radiocarbon dating. Palaeogeogr. Palaeoclimatol. Palaeoecol. 654, 112438. https://doi.org/10.1016/j.palaeo.2024.112438.

Pampaloni, M.L., Pichezzi, M.R., Raffi, I., Rossi, M., 1994. Calcareous planktonic biostratigraphy of the marne a *Orbulina* Unit (Miocene, Italy). G. Geol. 56, 139–153. https://doi.org/10.13130/2039-4942/6277.

Patacca, E., Scandone, P., 1989. Post-Tortonian mountain building in the Apennines. The role of the passive sinking of a relic lithospheric slab. Atti dei Convegni Lincei 80, 157–176.

Pedley, H.M., Bennett, S.M., 1985. Phosphorites, hardgrounds and syndepositional solution subsidence: a palaeoenvironmental model from the Miocene of the Maltese Islands. Sediment. Geol. 45, 1–34. https://doi.org/10.1016/0037-0738(85)90022-3.

Pennington, J.T., Chavez, F.P., 2000. Seasonal fluctuations of temperature, salinity, nitrate, chlorophyll and primary production at station H3/M1 over 1989–1996 in Monterey Bay, California. Deep-Sea Res. II Top. Stud. Oceanogr. 47, 947–973. https://doi.org/10.1016/S0967-0645(99)00132-0.

Perrin, C., 1992. Signification écologique des foraminifères acervulinidés et leur rôle dans la formation de faciès récifaux et organogènes depuis le Paléocène. Geobios 25, 725–751. https://doi.org/10.1016/S0016-6995(92)80054-H.

Pomar, L., 2001. Types of carbonate platforms: a genetic approach. Basin Res. 13, 313–334. https://doi.org/10.1046/j.0950-091x.2001.00152.x.

Pomar, L., Morsilli, M., Hallock, P., Bádenas, B., 2012. Internal waves, an under-explored source of turbulence events in the sedimentary record. Earth Sci. Rev. 111, 56–81. https://doi.org/10.1016/j.earscirev.2011.12.005.

Prager, E.J., Ginsburg, R.N., 1989. Carbonate nodule growth on Florida's outer shelf and its implications for fossil interpretations. Palaios 4, 310–317. https://doi.org/10.2307/3514555.

Pulecio-Plaza, L., Diaz-Pulido, G., García-Urueña, R., 2023. Seasonal upwelling conditions promote growth and calcification in reef-building coralline algae. J. Phycol. 59, 908–925. https://doi.org/10.1111/jpy.13370.

Purser, B.H., 1969. Syn-sedimentary marine lithification of Middle Jurassic limestones in the Paris Basin. Sedimentology 12, 205–230.

Quaranta, F., Tomassetti, L., Vannucci, G., Brandano, M., 2012. Coralline algae as environmental indicators: a case study from the Attard member (Chattian, Malta). Geodiversitas 34, 151–166. https://doi.org/10.5252/g2012n1a9.

Rehfeld, U., Janssen, A.W., 1995. Development of phosphatized hardgrounds in the Miocene *Globigerina* Limestone of the Maltese Archipelago, including a description of *Gamopleura melitensis* sp. nov. (Gastropoda, Euthecosomata). Facies 33, 91–106. https://doi.org/10.1007/BF02537445.

Reid, R.P., MacIntyre, I.G., 1988. Foraminiferal-algal nodules from the eastern Caribbean: growth history and implications on the value of nodules as paleoenvironmental indicators. Palaios 424–435.

Reiss, Z., Hottinger, L., 1984. The Gulf of Aqaba Ecological Micropaleontology. Ecological Studies, 50. Springer-Verlag. https://doi.org/10.1007/978-3-642-69787-6.

Ricci Lucchi, F., 1986. The Oligocene to recent foreland basins of the Northern Apennines. In: Allen, P.A., Homewood, P. (Eds.), Foreland Basins, International Association of Sedimentologists. Spec. Publ., 8. Blackwell Scientific Publications, Oxford, pp. 105–139.

Rosso, A., Gerovasileiou, V., Sanfilippo, R., Guido, A., 2019. Bryozoan assemblages from two submarine caves in the Aegean Sea (Eastern Mediterranean). Mar. Biodivers. 49, 707–726. https://doi.org/10.1007/s12526-018-0846-0.

Saderne, V., Wahl, M., 2013. Differential responses of calcifying and non-calcifying epibionts of a brown macroalga to present-day and future upwelling pCO_2. PLoS One 8, e70455. https://doi.org/10.1371/journal.pone.0070455.

Sañé, E., Chiocci, F.L., Basso, D., Martorelli, E., 2016. Environmental factors controlling the distribution of rhodoliths: an integrated study based on seafloor sampling, ROV and side scan sonar data, offshore the W-Pontine Archipelago. Cont. Shelf Res. 129, 10–22. https://doi.org/10.1016/j.csr.2016.09.003.

Sanfilippo, R., Rosso, A., Basso, D., Violanti, D., Di Geronimo, I., Di Geronimo, R., Benzoni, F., Robba, E., 2011. Cobbles colonization pattern from a tsunami-affected coastal area (SW Thailand, Andaman Sea). Facies 57, 1–13. https://doi.org/10.1007/s10347-010-0226-0.

Sanfilippo, R., Rosso, A., Guido, A., Mastandrea, A., Russo, F., Riding, R., Taddei Ruggiero, E., 2015. Metazoan/microbial biostalactites from present-day submarine caves in the Mediterranean Sea. Mar. Ecol. 36, 1277–1293. https://doi.org/10.1111/maec.12229.

Schlagintweit, F., Sanders, D., Studeny, M., 2018. The nepionic stage of *Solenomeris* Douvillé, 1924 (Acervulinidae, Foraminiferida): new observations from the uppermost Maastrichtian-early Danian of Austria (Kambühel Formation, Northern Calcareous Alps). Facies 64. https://doi.org/10.1007/s10347-018-0540-5.

Shannon, L.V., 1985. The Benguela ecosystem part I. Evolution of the Benguela, physical features and processes. Oceanogr. Mar. Biol. Ann. Rev. 23, 105–182.
Simone, L., Carannante, G., 1988. The fate of foramol ("temperate-type") carbonate platforms. Sediment. Geol. 60, 347–354. https://doi.org/10.1016/0037-0738(88)90129-7.
Smith, A.M., 2007. Age, growth and carbonate production by erect rigid bryozoans in Antarctica. Palaeogeogr. Palaeoclimatol. Palaeoecol. 256, 86–98. https://doi.org/10.1016/j.palaeo.2007.09.007.
Smith, A.M., 2014. Growth and calcification of marine bryozoans in a changing ocean. Biol. Bull. 226, 203–210. https://doi.org/10.1086/BBLv226n3p203.
Smith, A.M., Lawton, E.I., 2010. Growing up in the temperate zone: age, growth, calcification and carbonate mineralogy of *Melicerita chathamensis* (Bryozoa) in southern New Zealand. Palaeogeogr. Palaeoclimatol. Palaeoecol. 298, 271–277. https://doi.org/10.1016/j.palaeo.2010.09.033.
Sneed, E.D., Folk, R.L., 1958. Pebbles in the lower Colorado River, Texas a study in particle morphogenesis. J. Geol. 66, 114–150.
Spring, D.L., Williams, G.J., 2023. Influence of upwelling on coral reef benthic communities: a systematic review and metaanalysis. Proc. R. Soc. B 290, 20230023. https://doi.org/10.1098/rspb.2023.0023.
Steneck, R.S., 1986. The ecology of coralline algal crusts: convergent patterns and adaptative strategies. Annu. Rev. Ecol. Syst. 17, 273–303. https://www.jstor.org/stable/2096997.
Swezey, D.S., Bean, J.R., Hill, T.M., Gaylord, B., Ninokawa, A.T., Sanford, E., 2017. Plastic responses of bryozoans to ocean acidification. J. Exp. Biol. 220, 4399–4409. https://doi.org/10.1242/jeb.163436.
Tamega, F.T.S., Bassi, D., Figueiredo, M.A.O., Cherkinsky, A., 2014. Deep-water rhodolith bed from central Brazilian continental shelf, Campos Basin: coralline algal and faunal taxonomic composition. Galaxea J. Coral Reef Stud. 16, 21–31. https://doi.org/10.3755/galaxea.16.21.
Taylor, P.D., Wilson, M.A., 2002. A new terminology for marine organisms inhabiting hard substrates. Palaios 17, 522–525. https://doi.org/10.1669/0883-1351.
Torres, M.E., Embley, R.W., Merle, S.G., Trehu, A.M., Collier, R.W., Suess, E., Heeschen, K.U., 2009. Methane sources feeding cold seeps on the shelf and upper continental slope off central Oregon, USA. Geochem. Geophys. Geosyst. 10. https://doi.org/10.1029/2009GC002518.
Vale, N.F., Amado-Filho, G.M., Braga, J.C., Brasileiro, P.S., Kareza, C.S., Moraesa, F.C., Bahia, R.G., Bastos, A.C., Moura, R.L., 2018. Structure and composition of rhodoliths from the Amazon River mouth, Brazil. J. S. Am. Earth Sci. 84, 149–159. https://doi.org/10.1016/j.jsames.2018.03.014.
Vescogni, A., Vertino, A., Bosellini, F.R., Harzhauser, M., Mandic, O., 2018. New paleoenvironmental insights on the Miocene condensed phosphatic layer of Salento (southern Italy) unlocked by the coral-mollusc fossil archive. Facies 64, 7. https://doi.org/10.1007/s10347-018-0520-9.
Villas-Boas, A.B., de Riosmena-Rodriguez, R., Oliveira Figueiredo, M.A., 2014. Community structure of rhodolith-forming beds on the central Brazilian continental shelf. Helgol. Mar. Res. 68, 27–35. https://doi.org/10.1007/s10152-013-0366-z.
Walter, R.K., Woodson, C.B., Leary, P.R., Monismith, S.G., 2014. Connecting wind-driven upwelling and offshore stratification to nearshore internal bores and oxygen variability. J. Geophys. Res. Oceans 119, 3517–3534.
Walter, R.K., Stastna, M., Woodson, C.B., Monismith, S.G., 2016. Observations of nonlinear internal waves at a persistent coastal upwelling front. Cont. Shelf Res. 117, 100–117.
Weissert, H., Erba, E., 2004. Volcanism, CO_2 and palaeoclimate: a Late Jurassic–Early Cretaceous carbon and oxygen isotope record. J. Geol. Soc. Lond. 161, 695–702. https://doi.org/10.1144/0016-764903-087.
Wilson, J.L., 1975. Carbonate Facies in Geologic History. Springer Verlag, New York, p. 471.
Wissler, L., Funk, H., Weissert, H., 2003. Response of Early Cretaceous carbonate platforms to changes in atmospheric carbon dioxide levels. Palaeogeogr. Palaeoclimatol. Palaeoecol. 200, 187–205. https://doi.org/10.1016/S0031-0182(03)00450-4.
Woelkerling, W.J., Irvine, L.M., Harvey, A.S., 1993. Growth-forms in non-geniculate coralline red algae (Corallinales, Rhodophyta). Aust. Syst. Bot. 6, 277–293.
WoRMS Editorial Board, . World Register of Marine Species. Available from. https://www.marinespecies.org. at VLIZ. Accessed 2026-02-02. https://doi.org/10.14284/170.
Yilmaz, I.O., Altiner, D., Tekin, U.K., Ocakoglu, F., 2012. The first record of the "Mid-Barremian" Oceanic Anoxic Event and the Late Hauterivian platform drowning of the Bilecik platform, Sakarya Zone, western Turkey. Cretac. Res. 38, 16–39. https://doi.org/10.1016/j.cretres.2012.04.010.